

1 **Population genetics of *Glossina fuscipes fuscipes* from southern Chad**

2
3 Sophie Ravel¹, Mahamat Hissène Mahamat², Adeline Ségard¹, Rafael Argiles-Herrero³,
4 Jérémy Bouyer^{1,3,4,3}, Jean-Baptiste Rayaisse^{†5,4}, Philippe Solano¹, Brahim Guihini Mollo²,
5 Mallaye Pèka⁶Pèka^{†5}, Justin Darnas⁶Darnas⁵, Adrien Marie Gaston Belem⁷Belem⁶, Wilfrid
6 Yoni⁵Yoni⁴, Camille Noûs⁸Noûs⁷, Thierry de Meeûs^{1*}

7
8 ¹ Intertryp, IRD, Cirad, Univ Montpellier, Montpellier, France.

9 ² Institut de Recherche en Elevage pour le Développement (IRED), Ndjaména, Tchad.

10 ³ Insect Pest Control Laboratory, Joint Food and Agriculture Organization of the United
11 Nations/International Atomic Energy Agency Program of Nuclear Techniques in
12 Food and Agriculture, A-1400, Vienna, Austria.

13 ⁴~~CIRAD, UMR ASTRE CIRAD-INRA « AnimalS, health, Territories, Risks and~~
14 ~~Ecosystems », Campus international de Baillarguet, 34398 Montpellier cedex 05,~~
15 ~~France.~~

16 ⁵⁻⁴ Centre International de Recherche Développement sur l'Elevage en zone Subhumide
17 (Cirdes), Bobo-Dioulasso, Burkina Faso.

18 ⁶⁻⁵ Programme National de Lutte contre la THA (PNLTHA), Ndjaména, Tchad.

19 ⁷⁻⁶ Université Nazi Boni, Bobo-Dioulasso, Burkina Faso.

20 ⁸⁻⁷ Cogitamus laboratory, France, <https://www.cogitamus.fr/>.

21 E-mails: sophie.ravel@ird.fr; mahamatout@gmail.com; adeline.segard@ird.fr;

22 J.Bouyer@iaea.org; philippe.solano@ird.fr; Mollomodougou@yahoo.fr;

23 peka.mallaye@gmail.com; justindarnas@gmail.com; belemamq@hotmail.fr;

24 wilfridyoni@gmail.com; camille.nous@cogitamus.fr

25
26 * Correspondence: thierry.demeus@ird.fr (T. De Meeûs)

27
28 KeyWords: Tsetse flies, Dispersal, Trypanosomosis, Control.

29

30 **Abstract**

31 ~~In Sub-Saharan Africa, tsetse flies (genus *Glossina*) transmit deadly trypanosomes~~
32 ~~to human populations and domestic animals in sub-Saharan Africa; are vectors of~~
33 ~~trypanosomes causing~~ Human African ~~Trypanosomosis-Trypanosomiasis~~ (HAT) and
34 Animal African Trypanosomosis (AAT). Some foci of HAT persist in Southern Chad, where
35 a program of tsetse control was started against the local vector *Glossina fuscipes fuscipes*
36 in the Mandoul focus in 2014, and in Maro in 2018. Flies were also sampled in 2018 in
37 Timbéri and Dokoutou. We analyzed the population genetics of *G. fuscipes fuscipes* from
38 the four tsetse-infested zones. The trapping samples were characterized by a strong
39 female biased sex-ratio, except in Timbéri and Dokoutou that had high tsetse densities.
40 Apparent density and effective population density appeared smaller in the main foci of
41 Mandoul and Maro and the average dispersal distance (within the spatial scale of each
42 zone) was as large as or larger than the total length of each respective zone. The genetic
43 signature of a population bottleneck was found in the Mandoul and Timbéri area,
44 suggesting a large ancient interconnected metapopulation that underwent genetic
45 subdivision into small, isolated pockets due to adverse environmental conditions. The
46 long-range dispersal and the existence of genetic outliers suggest a possibility of migration
47 from remote sites such as the Central African Republic in the south (although the fly
48 situation remains unknown there) and/or a genetic signature of recent exchanges. Due to
49 likely isolation, an eradication strategy may be considered for sustainable HAT control in
50 Mandoul focus ~~and control can also be advised in the Dokoutou-Timbéri zone where HAT~~
51 ~~has not been reported yet but where AAT may cause problems on animal health~~. Another
52 strategy will probably be required in Maro focus, which ~~shows probably experiences~~ much
53 more exchanges with its neighbors.

54
55
56

57 **Introduction**

58 Tsetse flies (genus *Glossina*) transmit *Trypanosoma* spp. to humans and domestic
59 animals in sub-Saharan Africa, causing the devastating diseases Human African
60 Trypanosomosis (HAT) or sleeping sickness, and African Animal Trypanosomosis (AAT)
61 or nagana. There is no vaccine available against these diseases, and treatments are
62 difficult in humans and often compromised in animals due to the development of
63 resistance against the available trypanocidal drugs (Bouyer et al., 2009). The WHO aims
64 at interrupting transmission of *gambiense* HAT due to *Trypanosoma brucei gambiense* by
65 2030 (Büscher et al., 2018). Despite intensive disease surveillance programs and curative
66 treatments, some HAT foci persist in different countries in Sub-Saharan Africa. In the
67 southern part of Chad, medical surveillance and treatment has been supplemented with
68 control efforts against the main HAT vector *Glossina fuscipes fuscipes* since 2014 in the
69 Mandoul focus (Mahamat et al., 2017) and since 2018 in Maro (Ndung'u et al., 2020). The
70 use of insecticide-impregnated tiny targets has suppressed the tsetse population
71 significantly and resulted subsequently in a 63% decrease in HAT cases in the focus of
72 Mandoul (Mahamat et al., 2017). Nevertheless, to understand and predict the sustainability
73 of such vector control programs, it is necessary to study the biology of the vector
74 populations, in particular the size and connectivity of the different subpopulations and
75 dispersal capacities of the insects that drive reinvasion risks. This can be studied using
76 polymorphic genetic markers as microsatellite loci and population genetics tools (De
77 Meeûs et al., 2007). Such information can then be used to inform and develop the most
78 appropriate tsetse population management strategy, i.e. local eradication can be
79 considered if the tsetse target population is isolated- (Solano et al., 2010) (e.g. Solano et
80 al., 2010), whereas other situations would spur undertaking alternative control strategies.

81 Given the humidity and microhabitat requirements for the survival of *G. f. fuscipes*,
82 only the rivers with their riparian vegetation of the extreme South of Chad can sustain
83 populations of this fly. The remaining part of the country has a Sahel vegetation and hence
84 remains too dry for the survival of *G. f. fuscipes*. In this paper, we analyzed the population
85 genetics of several *G. f. fuscipes* populations that are infesting the southern part of Chad.
86 This included Mandoul and Maro, the main HAT foci of the country, but also Timbéri and
87 Dokoutou, where HAT cases were not reported. Nine microsatellite loci were used for a
88 population genetics analysis of a total sample of 205 tsetse flies to estimate effective
89 population density, dispersal distances and bottleneck signatures. The consequences of
90 these results are discussed in the context of a potential tsetse eradication program in this
91 area.

92

93 **Material and Methods**

94 *Ethical statement*

95 A prior informed consent (PIC) was obtained from the local focal point and a
96 mutually agreed terms (MAT) form was written and approved between Chadian
97 laboratories and French laboratories involved in the study for the use of the genetic
98 diversity found in tsetse flies from Chad.

99

100 *Origin of the samples*

101 All flies were captured with biconical-Challier-Laveissière traps (Challier &
102 Laveissière, 1973).

103 Sampling locations are described below and are presented in Figure 1. Details of
104 traps deployed in different sites and dates, and numbers of captured flies are presented in
105 the supplementary Figure S1. Detailed data with genotypes of individuals are available in
106 the supplementary File S1.

107 Mandoul and Maro are two active HAT foci. These two zones had to be sampled
108 and subjected to control at the same time, which required all logistic means. These zones
109 were thus studied one at a time. Later, Dokoutou and Timbéri, which are not HAT foci,
110 could then be sampled during the same season.

111 Number of sampled flies (females, males and total) per location and zone, the
112 cohort they belong to, taking two months as the generation time (De Meeûs et al., 2019)
113 are presented in Table 1.

114 It is important to note that during the surveys of 2018 that resulted in the sampling
115 of Timbéri and Dokoutou, no other tsetse flies were caught between Mandoul and these
116 localities despite trap deployment, meaning that the closest known geographic locality to
117 the Mandoul population, infested with tsetse flies, was ~50 km away as the crow flies (J.B.
118 Rayaisse, unpublished and Figure 1).

119

Commenté [SR1]: ???

Commenté [TDM2R1]: corrigé

120 Figure 1: Location of sampling zones (Dokoutou, Timbéri Mandoul and Maro), and traps
 121 (red crosses) for *Glossina fuscipes fuscipes* in Southern Chad. Cohorts and
 122 numbers of flies trapped are indicated in Table 1. Mandoul and Maro are active
 123 sleeping sickness foci. Main water courses are indicated with dashed blue lines and
 124 area subjected to flooding are represented by blue areas. Forest galleries are
 125 symbolized in grey.

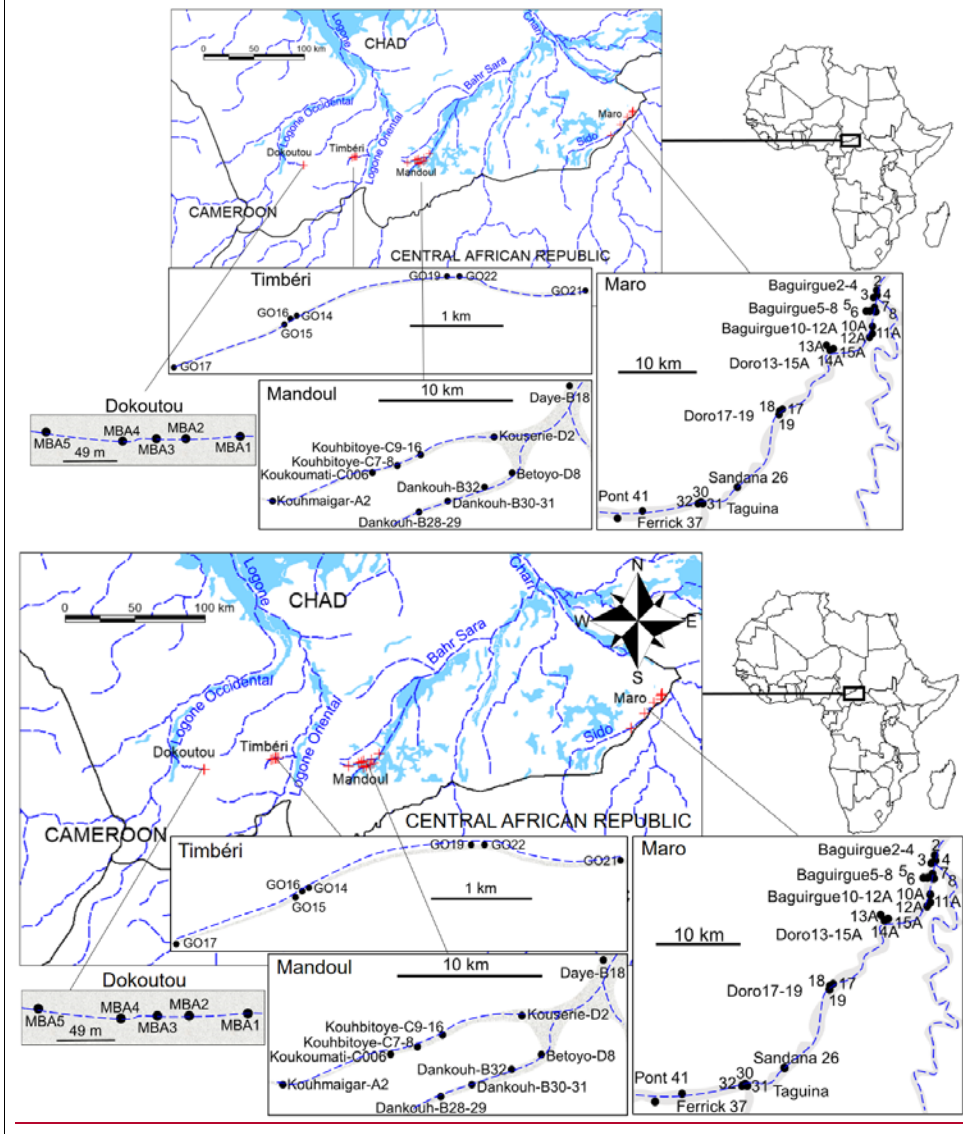


Table 1: FocusZone, cohort, number of females (N_f), males (N_m) and total number (N_t) of *Glossina fuscipes fuscipes* trapped in Southern Chad, and number of genotyped individuals (N_g). Cohorts were defined according to trapping dates, considering two months per *Glossina* generation (Mandoul November 2013 was cohort n°1; Maro April 2017, 42 months later i.e. 21 generations was n°22 and so on). The sex-ratio ($SR=N_m/N_f$) is also given, with exact p -value for significant deviation from even sex-ratio (two-sided exact binomial test).

<u>FocusZone</u>	Cohort	N_f	N_m	N_t	N_g	SR	p-value
Mandoul	C1	98	50	148	96	0.5102	<0.0001
Maro	C22	49	18	67	63	0.3673	0.0002
Timbéri	C32	12	10	22	19	0.8333	0.8318
Dokoutou	C32	12	15	27	27	1.25	0.7011
Total		171	93	264	205	0.5439	<0.0001

130

131 The significant deviation of the sex-ratio from 1 (even sex-ratio) was tested with a
 132 two-sided exact binomial test with R (R-Core-Team, 2020) (command "binom.test"). The
 133 significant variations of the sex-ratio from one site-zone to another were tested with
 134 Fisher's exact tests under the R-commander (rcmdr) package (Fox, 2005; Fox, 2007) for
 135 R. Densities of trapped flies (D_t) were computed for each focus-zone as the total number of
 136 flies captured (N_t , as defined in Table 1), divided by the surface of the polygon defined by
 137 the traps with at least one fly (S_p). Except for Dokoutou, this surface was computed with
 138 Karney's algorithm (Karney, 2013) with the package geosphere (command areaPolygon)
 139 (Hijmans et al., 2019) for R (see appendix 1). For Dokoutou, traps were deployed in a very
 140 short portion (213 m long) of the forest gallery. The attractive cone of a trap is known to be
 141 much bigger than that, i.e. with a radius of 200 m (Bouyer et al., 2015). We thus
 142 considered that the surface of this site was defined by the length of the sampling zone (i.e.
 143 213 m) plus twice the radius of the attractive cone (i.e. 2×200), hence 613 m, and a width
 144 corresponding to twice this radius, hence 400 m. This led to a surface of 0.2452 km²,
 145 which approximatively corresponds to the surface occupied by the dense vegetation found
 146 in this area.

147 Surfaces of zones were then 32.11, 226.74, 0.2452 and 1.37 km² for Mandoul,
 148 Maro, Dokoutou and Timbéri respectively.

149 The correlation between densities of captured flies (D_c) and sex-ratio (SR) was
 150 tested with a two-sided Spearman's rank correlation test under rcmdr.

151

152 *Microsatellite markers*

153 A total of nine di-nucleotidic microsatellite loci were used (GFF3, GFF4, GFF8,
154 GFF12, GFF16, GFF18, GFF21, GFF23, GFF27) with primers designed from a previously
155 built microsatellite bank of *G. f. fuscipes* (Ravel et al., 2020). All the markers selected were
156 autosomal (i.e. not on the X chromosome).

157

158 *Genotyping*

159 Legs from these flies were received in our lab in Montpellier. Three legs from each
160 of *G. f. fuscipes* individuals were subjected to chelex treatment as previously described
161 (Ravel et al., 2007) in order to obtain DNA for further microsatellite genotyping.

162 After PCR amplification of microsatellite loci, allele bands were routinely resolved on
163 ABI 3500XL sequencer. This method allows multiplexing by the use of four different dyes.
164 Allele calling was done using GeneMapper 4.1 software and the size standard GS600LIZ
165 short run. A total of 205 individuals were genotyped (Table 1).

166

167 *Structure of the data*

168 Data were sorted according to the cohort ($n^{\circ}1$, 22, and 32), considering two months
169 per generation, as routinely described in previous publications (e.g. see File S1 in (De
170 Meeûs et al., 2019)), traps ~~49 (49 traps in total)~~, then according to the sub-site as defined
171 in the Figure 1 (gathering traps that were less than 400 m apart) (see also Figure S1),
172 then sites (12 sites: Baguirgue, Betoyo, Dankouh, Daye, Dokoutou, Doro, Kouhbitoye,
173 Kouhmaigar, Koukoumati, Kouserie, Taguina and Timbéri), and zones (Mandoul, Maro,
174 Timbéri and Doukoutou) (Figure 1). Raw data are available in the supplementary file S1.

175 Except for analyses undertaken with HierFstat and sex biased dispersal (see
176 below), all genetic data were typed in the Create (Coombs et al., 2008) format and
177 converted by this software into the needed formats.

178

179 *Defining the relevant hierarchical levels of population structure*

180 Different hierarchical levels of population structure could be considered in Chadian
181 tsetse flies. In Mandoul, and Maro, we defined the Total sample, Sites, Subsites and
182 Traps, with their corresponding F_s : F_{SiteT} , $F_{SubsiteSite}$, and $F_{TrapSubsite}$. For the Timbéri and
183 Dokoutou, we could define the levels Total sample, Zone, Subsite and Trap, with the
184 corresponding F_{ZoneT} , $F_{SubsiteZone}$ and $F_{TrapSubsite}$. To measure and test the significance of
185 these hierarchical levels, we have used the algorithms implemented in HierFstat Package

186 (Goudet, 2005) for R. Hierarchical F -statistics estimate followed Yang's algorithm (Yang,
187 1998) and their significance was tested with 1000 randomizations of individuals between
188 traps within subsites, of traps between subsites within sites or zones, and of subsites
189 between sites or zones, to test the significant departure from 0 of $F_{\text{TrapSubsite}}$, $F_{\text{SubsiteSite}}$ Or
190 $F_{\text{SubsiteZone}}$, and F_{SiteT} or F_{ZoneT} respectively.

191 Because of the asynchrony of these samples, this needed to be undertaken in
192 Mandoul (cohort 1), Maro (cohort 22), and Timbéri-Dokoutou (cohort 32) separately (three
193 independent analyses).

194 More explanations and comments on hierarchical F -statistics can be found in (De
195 Meeûs & Goudet, 2007).

197 *Testing the quality of genetic markers and sampling*

198 We first studied the statistical independence of loci with the G -based test for linkage
199 disequilibrium (LD) across traps implemented in Fstat 2.9.4 (Goudet, 2003), updated from
200 (Goudet, 1995), with 10000 randomizations. This procedure is indeed the most powerful
201 way to combine tests across subsamples (De Meeûs et al., 2009). There are as many non-
202 independent tests as there are locus pairs (here 36 pairs). The 36 tests series were
203 adjusted with the Benjamini and Yekutieli (BY) false discovery rate (FDR) procedure for
204 non-independent tests series (Benjamini & Yekutieli, 2001) with R.

205 Deviation from local panmixia, absence of subdivision and deviation from global
206 panmixia were measured by Wright's F_{IS} , F_{ST} and F_{IT} respectively (Wright, 1965).
207 Interested readers can found more extensive definitions in (De Meeûs et al., 2007). These
208 were estimated with Weir and Cockerham's unbiased estimators (Weir & Cockerham,
209 1984) and their significance tested with 10000 randomizations of alleles between
210 individuals within subsamples (for panmixia), of individuals between subsamples (for
211 subdivision), and of alleles between individuals across the whole sample (global panmixia)
212 with Fstat. For these tests, the statistics used were the F_{IS} estimator, G (Goudet et al.,
213 1996) and F_{IT} estimator respectively. Default testing is unilateral (heterozygote deficit) for
214 F_{IS} and F_{IT} . The bilateral p -value was obtained by doubling the p -value if it was below 0.5,
215 or doubling $1-p$ -value otherwise. When needed, we compared F_{IS} and F_{IT} with a one-sided
216 ($F_{\text{IS}} < F_{\text{IT}}$) (unless specified otherwise) Wilcoxon signed rank test for paired data with
217 rcmdr. In that case, the pairing unit was the locus.

218 Jackknife over subsamples provided a standard error for F -statistics. This allowed
219 computing 95% confidence intervals (95%CI) of F -statistics as described in (De Meeûs et
220 al., 2007) to measure locus variation across subsamples. As it uses the student t

221 distribution (assuming normality, which is obviously not the case here), these 95%CI had
222 only an illustrative purpose. The 95%CI of F -statistics were also obtained with 5000
223 bootstraps over loci, as described in (De Meeûs et al., 2007). This procedure assumes no
224 particular distribution and thus have a statistical utility. We also computed standard error of
225 F_{IS} and F_{ST} from jackknives over loci, $StdErrFIS$ and $StdErrFST$ to be used for null
226 allele detection (seen Appendix 3).

227 In case of significant heterozygote deficit, we have looked for short allele
228 dominance (SAD), stuttering, null alleles and Wahlund effects as described in previous
229 studies (see Appendix 3).

230 LD tests, F -statistic estimates and testing, jackknives and bootstraps were
231 undertaken with Fstat 2.9.4 (Goudet, 2003) updated from (Goudet, 1995).

232

233 ~~Defining the relevant hierarchical levels of population structure~~

234 ~~———— Different hierarchical levels of population structure could be considered in Chadian~~
235 ~~testes flies. In Mandoul, and Maro, we defined the Total sample, Sites, Subsites and~~
236 ~~Traps, with their corresponding F_S , F_{SiteT} , $F_{SubsiteSite}$ and $F_{TrapSubsite}$. For the Timbéri and~~
237 ~~Dokoutou, we could define the levels Total sample, Zone, Subsite and Trap, with the~~
238 ~~corresponding F_{ZoneT} , $F_{SubsiteZone}$ and $F_{TrapSubsite}$. To measure and test the significance of~~
239 ~~these hierarchical levels, we have used the algorithms implemented in HierFstat Package~~
240 ~~(Goudet, 2005) for R. Hierarchical F statistics estimate followed Yang's algorithm (Yang,~~
241 ~~1998) and their significance was tested with 1000 randomizations of individuals between~~
242 ~~traps within subsites, of traps between subsites within sites or zones, and of subsites~~
243 ~~between sites or zones, to test the significant departure from 0 of $F_{TrapSubsite}$, $F_{SubsiteSite}$ or~~
244 ~~$F_{SubsiteZone}$ and F_{SiteT} or F_{ZoneT} respectively.~~

245 ~~———— Because of the asynchrony of these samples, this needed to be undertaken in~~
246 ~~Mandoul (cohort 1), Maro (cohort 22), and Timbéri-Dokoutou (cohort 32) separately (three~~
247 ~~independent analyses).~~

248 ~~———— More explanations and comments on hierarchical F statistics can be found in (De~~
249 ~~Meeûs & Goudet, 2007).~~

250

251 ~~Global level of subdivision~~ Population genetics structure regarding reproduction

252 Due to the temporal isolation between Mandoul, Maro and the Dokoutou-Timbéri
253 complex, these three samples were studied in specific paragraphs.

254 In some instance, we compared F_S and F_T with a one-sided Wilcoxon signed rank
255 test for paired data (the pairing object being the locus), under rcmdr, with H1 (alternative

256 hypothesis): $F_{IS} < F_{IT}$. We also used the same approach to compare F_{IS} within subsamples
257 (traps or subsites) with F_{IS_pooled} after the pooling of all tsetse flies into a single sample.
258 After correction for stuttering (when appropriate), null alleles, or more exactly
259 missing data (N_{blanks}) explained most of F_{IS} (or F_{IT}) variations. We then used the intercept
260 of the regression F_{IS} (or F_{IT}) $\sim N_{blanks}$ as an estimate of the basic F_{IS} of the population in
261 absence (or quasi-absence) of null alleles.

Mis en forme : Indice

Mis en forme : Non Exposant/ Indice

263 Global subdivision

Mis en forme : Police :Italique

264 Because of the presence of null alleles, F_{ST} was estimated with the ENA correction
265 with FreeNA (Chapuis & Estoup, 2007), for which we recoded missing data as
266 homozygous for null alleles (coded 999, as recommended). We labelled this new estimate
267 as F_{ST_FreeNA} . Confidence intervals of these estimates were computed after 5000
268 bootstraps over loci.

269 ~~Because~~ For microsatellite loci, because of high mutation rates and excesses of
270 polymorphism that results from it, the maximum possible value is lower than unity for F_{ST}
271 ($F_{ST_max} < 1$) in microsatellite loci (Hedrick, 2005b). To correct this estimate for excess of
272 polymorphism, we can divide the actual estimator by the maximum possible value given
273 the polymorphism observed within subsamples (Meirmans, 2006), or use $G_{ST}'' = [n(H_T -$
274 $H_S)] / [(nH_T - H_S)(1 - H_S)]$ (Meirmans & Hedrick, 2011). Wang's criterion (Wang, 2015) allows
275 determining which of the two approaches is more appropriate. If the correlation between
276 Nei's G_{ST} and H_S is strongly negative, then F_{ST} based standardizations are more accurate,
277 otherwise G_{ST}'' should be used. This was tested with a one-sided Spearman's rank
278 correlation test under rcmdr. We computed the standardized estimator of F_{ST} using
279 Recodedata (Meirmans, 2006) to compute a maximum possible $F_{ST_FreeNA_max}$. We then
280 obtained the standardized $F_{ST_FreeNA}' = F_{ST_FreeNA} / F_{ST_FreeNA_max}$. In that case, we obtained
281 95%CI with 5000 bootstraps over loci. These standardized subdivision measures could
282 then be used to compute the effective number of immigrants within subpopulations as
283 $N_e m = (1 - F_{ST}') / (4F_{ST}')$, where F_{ST}' stands for G_{ST}'' or F_{ST_FreeNA}' (depending on Wang's
284 criterion), or $N_e m = (1 - F_{ST}') / (8F_{ST}')$, in the special case of two subpopulations (i.e. Timbéri
285 and Dokoutou ~~sites~~) (e.g. (De MeeÛs, 2012), page 50).

287 Isolation by distance

288 Except for the Timbéri-Dokoutou sites for which captures were done the same year,
289 isolation by distance was tested inside each zone separately. It was measured and tested
290 with Rousset's model of regression in two dimensions $F_{ST_R} = a + b \times \ln(D_{Geo})$ (Rousset,

291 1997). In this equation, $F_{ST,R} = F_{ST}/(1-F_{ST})$ is Rousset's genetic distance between two
292 subsamples (traps), a and b are the intercept and the slope of the regression respectively,
293 and $\ln(D_{Geo})$ is the natural logarithm of the geographic distance between the two traps.
294 Geographic distances were computed with the command `distGeo` of the package
295 `geosphere` of R (see Appendix 1). The significance of the regression was tested by 5000
296 bootstraps over loci that provided a 95%CI of the slope. Because null alleles were present,
297 we recoded all blank genotypes as homozygous profiles for allele 999 and used the ENA
298 correction as recommended (Chapuis & Estoup, 2007) to compute $F_{ST-FreeNA}$. This was
299 undertaken with FreeNA (Chapuis & Estoup, 2007). In case of significance, the
300 neighborhood size and number of immigrants coming from neighbors and entering a
301 subpopulation at each generation (in two dimensions) was computed as $Nb = 4\pi D_e \bar{\sigma}^2 = 1/b$,
302 and $N_e m = 1/(2\pi b)$ respectively (Rousset, 1997; Watts et al., 2007). In these formulae, D_e is
303 the effective population density, $\bar{\sigma}^2$ is the average of squared axial distances between
304 adults and their parents, and b is the slope of Rousset's regression model for isolation by
305 distance (Rousset, 1997).

306 Some subsamples harbored too few individuals that could not be taken into account
307 in isolation by distance between traps or even subsites. We thus also undertook isolation
308 by distance between individuals with Genepop 4.7.0 (Rousset, 2008), with the parameter \hat{e}
309 (Watts et al., 2007) for the genetic distance if not specified otherwise (i.e. when $Nb > 50$),
310 and 1000000 randomizations for the Mantel test. Note that in that case, no correction for
311 null alleles was possible. In case of non-significance with previous procedures, we also
312 undertook a Mantel test using the Cavalli-Sforza and Edwards' chord distance $D_{CSE-FreeNA}$
313 (Cavalli-Sforza & Edwards, 1967), computed with the INA correction for null alleles
314 (Chapuis & Estoup, 2007) with FreeNA, and 10000 randomizations with the "Mantelize it"
315 menu of Fstat. This genetic distance can indeed prove more powerful in case of weak
316 signals (Séré et al., 2017). Mantel test in Fstat is two sided. We thus computed the one-
317 sided p -value as half the p -value obtained for a positive correlation or $(1-p\text{-value})/2$
318 otherwise.

319 *Effective population sizes*

321 For these computations, subsample units used were defined by the results obtained
322 with HierFstat. In case of suspicion of a weak population subdivision, like in Mandoul and
323 Maro foci, we also used the whole corresponding zone as a single unit. Effective
324 population sizes were estimated with four different methods. The first method was the
325 linkage disequilibrium (LD) method (Waples, 2006) adjusted for missing data (Peel et al.,

Code de champ modifié

2013), and the second method was the coancestry method (Nomura, 2008). These two methods were both implemented with NeEstimator version 2.1 (Do et al., 2014). The third method was the within and between loci correlations (Vitalis & Couvet, 2001b) computed with Estim 1.2 (Vitalis, 2002) updated from (Vitalis & Couvet, 2001a). The fourth method was the heterozygote excess method from Balloux (Balloux, 2004). For the LD method, we retained only data with minimum allele frequency 0.05 as recommended in NeEstimator manual. We averaged N_e across usable values (excluding "infinite" results). We also retained minimum and maximum values across the four methods used. We finally computed the grand average and average minimum and maximum N_e across methods.

335

336 *Effective population densities*

337 All the four zones investigated are quite isolated from each other's: in time, by at
338 least 10 generations, and in space, by at least 50 km for all, except between Dokoutou and
339 Timbéri, which are spatially isolated from each other's by 50 km, but are
340 contemporaneous.

341 Computing the effective population density in a given zone X ($D_{e\ X}$) needs a
342 knowledge of the relevant surface S_X , on which computing the total effective population
343 size on that surface $N_{e\ X}$, so that $D_{e\ X} = N_{e\ X} / S_X$.

344 We adapted the estimate of total effective population sizes to what was observed in
345 each zone.

346 When no or weak population subdivision occurred, then each subsample was
347 considered as a representative of the total zone and the average N_e was used as $N_{e\ X}$.
348 This is what we observed within all four zones.

349 When a significant subdivision occurred, as between Dokoutou and Timbéri,
350 several quantities were computed. In Mandoul, the average effective population size over
351 subsites was multiplied by the number of subsites to obtain the total $N_{e\ T}$, we also used the
352 estimates obtained over all the focus. In Maro, the average N_e across traps, or computed
353 over all the focus was used to estimate $N_{e\ T}$. For Dokoutou and Timbéri, separately, we
354 used the global N_e of each zone. The effective population densities were thus computed
355 as $N_{e\ T} / S$, where S is the surface of the zone, as computed above with the command
356 "areaPolygon" of the package geosphere of R. No other population of tsetse flies were
357 met between these two zones. For Consequently, for the effective population density
358 across Dokoutou and Timbéri, we summed the two N_e obtained in each of the two zones
359 to obtain $N_{e\ \text{DokoutouTimbéri}}$, and the surface $S_{\text{DokoutouTimbéri}}$ was assumed to correspond to
360 the disc defined by the distance between these two zones (D_{geo}) as the diameter of this

Mis en forme : Pas de paragraphes solidaires

361 disc, i.e. $S_{DokoutouTimbéri} = \pi \times (D_{geo}/2)^2$. When considering isolation by distance across traps of
362 both zones, we computed this surface using the GPS coordinates of all traps of both zones
363 with the package `geosphere` for R (command `areaPolygon`) (S_{DT_Area}). The effective
364 population density was then obtained as $D_{e-DokoutouTimbéri} = N_{e-DokoutouTimbéri} / S_{DokoutouTimbéri_X}$,
365 where X stands for Disc or Area.

366 *Isolation by distance*

367 ——— Except for the Timbéri-Dokoutou sites for which captures were done the same year,
368 isolation by distance was tested inside each zone separately. It was measured and tested
369 with Roussot's model of regression in two dimensions $F_{ST_R} = a + b \times \ln(D_{Geo})$ (Roussot,
370 1997). In this equation, $F_{ST_R} = F_{ST} / (1 - F_{ST})$ is Roussot's genetic distance between two
371 subsamples (traps), a and b are the intercept and the slope of the regression respectively,
372 and $\ln(D_{Geo})$ is the natural logarithm of the geographic distance between the two traps.
373 Geographic distances were computed with the command `distGeo` of the package
374 `geosphere` of R (see Appendix 1). The significance of the regression was tested by 5000
375 bootstraps over loci that provided a 95% CI of the slope. Because null alleles were present,
376 we recoded all blank genotypes as homozygous profiles for allele 999 and used the ENA
377 correction as recommended (Chapuis & Estoup, 2007) to compute F_{ST_FreeNA} . This was
378 undertaken with `FreeNA` (Chapuis & Estoup, 2007). In case of significance, the
379 neighborhood size and number of immigrants coming from neighbors and entering a
380 subpopulation at each generation (in two dimensions) was computed as $N/b - 4\pi D_e \bar{\sigma}^2 - 1/b$,
381 and $N_e m = 1/(2\pi b)$ respectively (Roussot, 1997; Watts et al., 2007). In these formulae, D_e is
382 the effective population density, $\bar{\sigma}^2$ is the average of squared axial distances between
383 adults and their parents, and b is the slope of Roussot's regression model for isolation by
384 distance (Roussot, 1997).

385 ——— Some subsamples harbored too few individuals that could not be taken into account
386 in isolation by distance between traps or even subsites. We thus also undertook isolation
387 by distance between individuals with `Genopop` 4.7.0 (Roussot, 2008), with the parameter $\hat{\epsilon}$
388 (Watts et al., 2007) for the genetic distance if not specified otherwise (i.e. when $N/b > 50$),
389 and 1000000 randomizations for the Mantel test. Note that in that case, no correction for
390 null alleles was possible. In case of non-significance with previous procedures, we also
391 undertook a Mantel test using the Cavalli-Sforza and Edwards' chord distance D_{CSE_FreeNA}
392 (Cavalli-Sforza & Edwards, 1967), computed with the INA correction for null alleles
393 (Chapuis & Estoup, 2007) with `FreeNA`, and 10000 randomizations with the "Mantelize it"
394 menu of `Estat`. This genetic distance can indeed prove more powerful in case of weak
395

Code de champ modifié

396 ~~signals (Séré et al., 2017). Mantel test in Fstat is two sided. We thus computed the one-~~
397 ~~sided p value as half the p value obtained for a positive correlation or (1 - p value)/2~~
398 ~~otherwise.~~

399

400 *Dispersal distances*

401 The average distance between adults and their parents was extracted with the
402 equation (e.g. (De Meeûs et al., 2019)):

$$403 \quad \delta \approx 2 \sqrt{\frac{1}{4\pi b D_e}}$$

404 In this equation, b is the slope of Rousset's regression for isolation by distance and
405 D_e is the average effective population density. This quantity is only accurate when
406 dispersal distances follow a symmetrical distribution with a strong kurtosis. In any other
407 case, like skewed distributions (right or left), or platykurtic distributions, δ will be slightly
408 overestimated. Since there is also a lack of accuracy for D_e , δ corresponded more to an
409 order of magnitude than a precise estimate of dispersal distance.

410 ~~_____ In the special case of Dokoutou-Timbéri meta-zone, we had the opportunity to~~
411 ~~compute this distance using quasi-independent methods. The first method used the F_{ST} '~~
412 ~~based estimate of m (immigration rate) between the two zones, the average distance~~
413 ~~between these (D_{DT}) to get $\delta_m = m \times D_{DT}$. The second method used the slope b_{All} of isolation~~
414 ~~by distance between traps across the two zones and the S_{DT_Area} based estimate of D_{e-DT}~~
415 ~~to obtain δ_{b_All} with the formula above. The third used the slope b_{Within} of isolation by~~
416 ~~distance within each zone and the corresponding surface defined above for each zone,~~
417 ~~and computed δ_{b_Within} . We also used individual, trap, and subsite based isolation by~~
418 ~~distance parameters to obtain various estimates of δ . This allowed checking for the~~
419 ~~consistency between the different values obtained. Individual-based isolation by distance~~
420 ~~does not correct for null alleles and thus is expected to produce overestimated and more~~
421 ~~variable slopes.~~

422 ~~_____ We also used the census of captured flies in traps to compute census population~~
423 ~~densities of captured flies (not the census population size) within each zone.~~

424

425 *Factorial components analysis (FCA), DAPC and NJTree analyses*

426 In order to visualize how the genetic information of the different individuals distribute
427 relative to each other's, we have undertaken a factorial correspondence analysis (FCA)
428 (She et al., 1987), where the values of inertia along each principal axis can be seen as F_{ST}

Mis en forme : Non Exposant/ Indice

Mis en forme : Police :Italique

429 combinations of different loci (Guinand, 1996). This analysis was undertaken with Genetix
430 (Belkhir et al., 2004). Significance of the axes was assessed with the broken stick criterion
431 (Frontier, 1976). We have also undertaken a DAPC analysis (Jombart et al., 2010), with
432 the adegenet package (Jombart, 2008) for R. We finally computed a neighbor joining tree
433 (NJTree) (Saitou & Nei, 1987) between sites, based on a Matrix of Cavalli-Sforza and
434 Edwards chord distance (Cavalli-Sforza & Edwards, 1967), D_{CSE} as recommended
435 (Takezaki & Nei, 1996). The matrix was computed with the INA correction of FreeNA to
436 correct for null alleles, with missing data recoded as homozygotes for allele 999 as
437 recommended (Chapuis & Estoup, 2007), and the NJTree built with MEGA 7 (Kumar et al.,
438 2016). To test for the respective effects of geographic and temporal distances on genetic
439 distances of this tree, we also undertook a partial Mantel test (Manly, 1997) with Fstat
440 2.9.4, based on the absolute regression coefficients and 10000 randomizations. In Fstat,
441 p -values are two sided, but here we expected a positive correlation. One-sided p -values
442 were thus obtained by halving p -values of positive correlations, and computing $1-(p$ -
443 value)/2 otherwise.

444

445 *Sex specific genetic structure*

446 To test for the existence of a sex specific genetic structure, we used the biased
447 dispersal menu of Fstat. We studied this in the four samples separately (namely in
448 Mandoul C1, Maro C22, and Timbéri-Dokoutou C32). To gain in power and have enough
449 males and females per subsample, we considered the subsites, as defined earlier, as
450 subpopulation units. We used the corrected average assignment index $mAlc$, the variance
451 of this index $vAlc$ and Weir and Cockerham's unbiased estimate of F_{ST} , as recommended
452 (Goudet et al., 2002; Prugnolle & De Meeûs, 2002) with 10000 permutations of gender
453 status within subsamples. Significant male biased dispersal was seldom found in tsetse
454 flies: once in *G. palpalis palpalis* in Cameroon (Mélachio et al., 2011), and twice for *G.*
455 *tachinoides* in Burkina-Faso (Kone et al., 2011; Ravel et al., 2013). We thus used one-
456 sided tests for male biased dispersal with the alternative hypotheses (subscript F and M
457 designating female and male parameters respectively): $mAlc_F > mAlc_M$; $vAlc_F < vAlc_M$; and
458 $F_{STF} > F_{STM}$. Here, correction for null alleles was not possible, and alleles needed to be
459 recoded with two digits. For each parameter, there are three tests (the three cohorts: C1,
460 C22, C32). For each parameter tested, we combined the p -values obtained across cohorts
461 with the generalized binomial procedure (Teriokhin et al., 2007) computed with MultiTest
462 v1.2 (De Meeûs et al., 2009) and following the rules described in the user guide: using
463 $K=k/2$ if $k>3$, and $K=k$ otherwise, where k is the number of tests to be combined and K is

464 the subset of smallest p -values to be considered. More explanations can be found
465 elsewhere (De Meeûs, 2014).

466

467 *Bottleneck detection*

468 We used the algorithm developed by Cornuet and Luickart (Cornuet & Luickart,
469 1996) to detect the signature of a recent bottleneck in the different subsamples. We used
470 the unilateral Wilcoxon test as recommended by the authors. As suggested ((De Meeûs,
471 2012), pages 104-105) , we studied IAM, TPM with default values (i.e. 70% of SMM and a
472 variance of 30), and SMM models of mutation. A bottleneck signature likely occurred when
473 the test is highly significant with IAM, and significant at least with TPM. Alternatively, a
474 slightly significant bottleneck signature only observed with IAM more probably reflects
475 small effective subpopulations sizes. We used Bottleneck v 1.2.02 (Piry et al., 1999) to
476 undertake these tests in each cohort separately. The p -values obtained were combined
477 across subsamples with the generalized binomial procedure, to get a global picture. We
478 also used the Figure 3 in (Cornuet & Luickart, 1996) to extrapolate the probable post and
479 pre bottleneck effective population sizes ($N_{e\text{-post}}$ and $N_{e\text{-pre}}$ respectively), using the
480 probable $\tau=g/(2N_{e\text{-post}})$ and $\alpha= N_{e\text{-pre}}/N_{e\text{-post}}$, where g is the number of generations after the
481 bottleneck event, and given the number of loci (here $9\approx 10$), their genetic diversity (H_s) and
482 sample size (N_{sample}) used.

483

484 **Results**

485 *Sex-ratio within and between foci*

486 There was a global and highly significant biased sex-ratio in favor of females (Table
487 1). This sex-ratio significantly varied between the different zones (p -value=0.0469).
488 Densities of flies trapped in Mandoul, Maro, Dokoutou and Timbéri were 4.6, 0.3, 110.1,
489 and 16, flies/km², respectively. Variation of effective population density across sites was
490 strongly positively correlated with densities of capture ($\rho=1$), but marginally not
491 significantly so (p -value=0.0833, two-sided). However, with four points, this p -value was in
492 fact the minimum possible one.

493

494 *Defining the relevant hierarchical levels of population structure*

495 The results of this approach are presented in Table 2. Scripts and detailed results
496 are presented in Appendix 2. It can be seen that population genetic structure did not occur
497 at the same scale for the different sites/foci. In Mandoul, only the subsites displayed a
498 significant effect. In Maro, only traps mattered. In Timbéri and Dokoutou, the zone

499 mattered most, but not significantly so. Nevertheless, when only levels Trap and Zone
 500 were kept, $F_{\text{ZoneTotal}}=0.0867$ with $p\text{-value}=0.002$. Moreover, signals were quite small in
 501 Mandoul and Maro (Table 2). This will need to be further explored.

502

503 Table 2: Results of the hierarchical F -statistics with HierFstat of the different samples for
 504 *Glossina fuscipes fuscipes* from Chad. The effect of subsites was measured within
 505 each site in Mandoul and Maro and within each zone for Timbéri and Dokoutou. For
 506 each sample, most important level is in bold.

Effect	Sample	Mandoul	Maro	Timbéri-Dokoutou
Zone	F_{ZoneT}			0.075
	$p\text{-value}$	NA	NA	0.196
Sites	F_{SiteT}	0.000	-0.007	NA
	$p\text{-value}$	0.303	0.567	
Subsites	$F_{\text{SubsiteSite/Zone}}$	0.018	0.000	0.020
	$p\text{-value}$	0.025	0.656	0.660
Traps	$F_{\text{TrapSubsite}}$	-0.027	0.005	-0.020
	$p\text{-value}$	0.720	0.031	0.961

507

508

509 *Testing the quality of genetic markers and sampling*

510 Detailed analyses were quite fastidious and are presented in Appendix 3.

511 No signature of any linkage disequilibrium could be detected and all loci were
 512 considered as statistically independent in all zones.

513 No SAD signature could be found in any of the four zones. Null alleles were present
 514 in all samples at several loci and corrected accordingly. Stuttering was found at several
 515 loci in Maro, Timbéri and Dokoutou and correction applied as described in Appendix 3.

516 There was no evidence of any Wahlund effect in any of the four zones.

517

518 *Population genetics structure regarding reproduction of tsetse flies from Mandoul*

519 Due to null alleles, the global $F_{\text{IS}}=0.128$ in 95%CI=[0.039, 0.243], was significantly
 520 different from 0 ($p\text{-value}<0.0002$). Population structure was weak, with a small and
 521 marginally not significant $F_{\text{ST}}=0.005$ in 95%CI=[-0.007, 0.016] ($p\text{-value}=0.0722$).

522 Interestingly, $F_{\text{IT}}=0.132$ in 95%CI=[0.047, 0.244] was not significantly different from the F_{IS}
 523 ($p\text{-value}=0.2129$). It is thus possible that the whole focus behaves as a single pangamic

524 population. Now, considering the whole focus as a single population, only two locus pairs

525 appeared in significant LD (p -values=0.0084 and 0.0344), none of which remained
526 significant after BY adjustment (all p -values=1), and the F_{IS} =0.13 in 95%CI=[0.045, 0.238],
527 was not significantly bigger than within subsites (p -value=0.3594) (no statistically
528 detectable Wahlund effect). Again, missing data explained very well the positive F_{IS}
529 (ρ =0.6836, p -value=0.0212, R^2 =0.5733), with a residual F_{IS-res} =-0.0493.

530 _____ Using F_{IS} or F_{IT} regressions against number of missing genotypes (Appendix 3), the
531 intercept was used to estimate the residual values in absence of null alleles, which were
532 F_{IS-res} =-0.0547 and F_{IT-res} =-0.0474.

534 Global subdivision in Mandoul

535 With FreeNA, the corrected subdivision measure was bigger than the uncorrected
536 one: F_{ST_FreeNA} =0.0192 in 95%CI=[0.0084, 0.0295].

537 _____ The correlation between G_{ST} and H_S was strongly negative (ρ =-0.7833, p -
538 value=0.0086). Recodedata (Meirmans, 2006) provided $F_{ST_FreeNA-max}$ =0.2691 in
539 95%CI=[0.2086, 0.3410]. Consequently, F_{ST_FreeNA}' =0.0713 in 95%CI=[0.0405, 0.0866].
540 Some subdivision was observed, but given the correspondence between F_{IS} and F_{IT} it was
541 at best weak.

543 Isolation by distance in Mandoul

544 Isolation by distance between subsites provided a very small and not significant
545 slope b =0.0088 in 95%CI=[-0.0303, 0.0407]. The \hat{e} -based isolation by distance between
546 individuals did not provide a different conclusion: b =0.0016 in 95%CI=[-0.0039, 0.0082]
547 (Mantel test p -value=0.3178) (~~$Nb=607 >> 50$~~). When using D_{CSE} , the Mantel test provided a
548 highly significant correlation (p -value=0.0003), with a very small coefficient of
549 determination (R^2 =0.0776). Isolation by distance thus occurred, but with a very weak
550 signal. This would be in line for the existence of a nearly pangamic unit at the focus scale
551 for Mandoul. Parameters' estimate from isolation by distance between subsites yielded a
552 neighborhood Nb =114 individuals and an effective number of immigrants from neighbor
553 sites $N_e m$ =18 individuals per generation. For isolation by distance between individuals, the
554 neighborhood obtained was Nb =607 individuals and $N_e m$ =97 individuals per generation.

555 _____ ~~Now, considering the whole focus as a single population, only two locus pairs~~
556 ~~appeared in significant LD (p -values=0.0084 and 0.0344), none of which remained~~
557 ~~significant after BY adjustment (all p -values=1), and the F_{IS} =0.13 in 95%CI=[0.045, 0.238],~~
558 ~~was not significantly bigger than within subsites (p -value=0.3594) (no Wahlund effect).~~
559 ~~Again, missing data explained very well the positive F_{IS} (ρ =0.6836, p -value=0.0212,~~

Mis en forme : Police :Italique

Mis en forme : Police :Italique

560 $R^2=0.5733$), with a residual $F_{IS-res}=-0.0493$. Hence, pooling all individuals into a single unit
561 did not produce any Wahlund effect. This would be in line for the existence of a nearly
562 panmictic unit at the focus scale for Mandoul.

564 Effective population size in Mandoul

Mis en forme : Police :Italique

565 Effective population sizes were computed within each subsite containing enough
566 individuals (i.e. at least 7 individuals) or within the whole focus as a single population. Only
567 two subsites provided usable values with the LD method (DankouhB30-31 and
568 DankouhB28-29) and the coancestry method (DankouhB32 and DankouhB28-29), and
569 only one with Estim (Betoyo). For Balloux' method, we used the residual F_{IS-r} computed
570 with the missing genotype/ F_{IS} regression. The average effective subsite size was $N_e=50$ in
571 minimax=[9, 153] individuals. When we considered the whole focus as a single population,
572 $N_e=141$ in minimax=[10, 272]. This is obviously not different from subsite-based estimate,
573 though much more variable due to a lack of replicates. We thus kept within subsites
574 averaged values.

576 Effective population densities in Mandoul

Mis en forme : Police :Italique

577 The average surface of subsites was $S_{subsites}=3304\text{ m}^2$, and its surface of Mandoul
578 was $S_{Mandoul}=32\text{ km}^2$ for the whole focus. This led to very different effective population
579 densities: $D_{e-subsites}=15111$ in minimax=[2784, 46288] individuals/ km^2 , and $D_{e-Mandoul}=4.41.6$
580 in minimax=[0.3, 8.547.6] individuals/ km^2 . More than 15000 individuals/ km^2 did not
581 correspond to field observations and the whole zone obviously represents a more accurate
582 scale.

584 Dispersal distances in Mandoul

Mis en forme : Police :Italique

585 Using $D_{e-Mandoul}$, we obtained two different effective dispersal distances:
586 $\bar{\sigma}_{subsites}=2870.4823$ m in minimax=[2067871, 4067511237] m/generation, for the subsite
587 based isolation by distance regression; and $\bar{\sigma}_{individuals}=6634.11149$ in minimax=[20144778,
588 2467625976] m/generation for the individual based isolation by distance regression. The
589 two methods provided largely overlapping values. For information, the two most distant
590 traps that captured at least one fly were 24 km distant from each other's in that focus.

591
592 Population genetics structure regarding reproduction of tsetse flies from Maro after
593 corrections for stuttering

594 After correction for stuttering at loci Gff3, 12, 16, 18 and Gff27 (Appendix 3), there
595 was a non-significant and weak heterozygote excess within traps ($F_{IS}=-0.001$ in 95%CI=[-
596 0.045, 0.036], p -value=0.9268). Null alleles affected weakly the data, with $p_{null}=0.0585$,
597 and nine missing genotypes for Gff4 and much less for other loci.

598

599 Global subdivision in Maro

600 Subdivision was very small and not significant: $F_{ST}=0.003$ in 95%CI=[-0.01, 0.019]
601 (p -value=0.135). This suggested again that tsetse flies from Maro almost behaved as a
602 single population. Indeed, when pooling all individuals into one single unit, we observed
603 only one significant LD locus pair (not significant after BY correction), and a $F_{IS}=0.001$ in
604 95%CI=[-0.035, 0.034], that was not significantly greater than the initial one (p -
605 value=0.2852, ~~one-sided test~~). Nevertheless, with FreeNA estimates, $F_{ST-FreeNA}=0.0182$ in
606 95%CI=[0.0017, 0.0419] was significantly above 0. The correlation between H_S and G_{ST}
607 was not significantly negative ($\rho=0.1333$, p -value=0.646, one sided test), nevertheless,
608 $G_{ST}''=0.0479$ (without 95%CI) was almost the same as the value obtained with Meirmans'
609 method: $F_{ST-FreeNA}'=0.0434$ in 95%CI=[0.0069, 0.0716]. There was thus a possibility for a
610 feeble subdivision signature with a global number of effective immigrants (using Meirmans
611 estimates) $N_e m=5.06$ on average and overall the focus.

612

613 Isolation by distance in Maro

614 Isolation by distance between traps, using F_{ST} estimates with the ENA correction
615 computed with FreeNA, and after recoding missing data as null homozygotes, was not
616 significant with the bootstrap 95%CI of the slope of Rousset's regression: $b=0.0074$ in
617 95%CI=[-0.00024, 0.0169]. However, the Mantel test based on geographic distances and
618 $D_{CSE-FreeNA}$ was highly significant (one sided p -value=0.0002). Finally, isolation by distance
619 between individuals with Genepop (and no correction for null alleles), yielded a negative
620 slope. So, at best, isolation by distance was weak and dispersal distances were probably
621 substantial, and may be close or equal to the maximum length of the zone defined by Maro
622 (32.4 km).

623

624 Effective population size of Maro

625 Effective population sizes computations did not output many values within traps:
626 one with the LD method, two with the coancestry method, and five with Balloux's method
627 (i.e. the five loci with a heterozygous excesses). It averaged $N_{e_traps}=55$ in minimax=[17,
628 118]. For the focus taken as a whole, only coancestry (one value) and Balloux's methods

Mis en forme : Police :Italique

Mis en forme : Police :Italique

629 (five values) provided usable values. The average was $N_{e-focus}=28$ in $minimax=[20, 36]$,
630 which was quite convergent with the previous values, confirming that the right scale ~~may~~
631 ~~be~~was the focus. We thus kept the trap-based estimate.

632

633 Effective population density in Maro

634 _____ The area occupied by traps with at least one fly corresponded to a surface
635 ~~$S_{focus, S_{Maro}} \approx 227$ km². This yielded to very small effective population densities in the focus~~
636 ~~$D_{e-focus}=0.24$ in $minimax=[0.08, 0.52]$ individuals per km² for traps, and $D_{e-focus}=0.12$ for~~
637 ~~subsites and whole focus estimates, in $minimax=[0.09, 0.16]$ individuals per km².~~

638 _____ ~~Isolation by distance between traps, using F_{ST} estimates with the ENA correction~~
639 ~~computed with FreeNA, and after recoding missing data as null homozygotes, was not~~
640 ~~significant with the bootstrap 95%CI of the slope of Rousset's regression: $b=0.0074$ in~~
641 ~~$95\%CI=[-0.00024, 0.0169]$. However, the Mantel test based on geographic distances and~~
642 ~~$D_{CSE-FreeNA}$ was highly significant (one-sided p -value=0.0002). Finally, isolation by distance~~
643 ~~between individuals with GenePop (and no correction for null alleles), yielded a negative~~
644 ~~slope. So, at best, isolation by distance was weak and dispersal distances were probably~~
645 ~~substantial, and may be close or equal to the maximum length of the zone defined by~~
646 ~~Maro.~~

647

648 Dispersal distances in Maro

649 ~~Using traps based estimate of density, †~~The average dispersal distance was
650 ~~$\delta_{traps}=13.7$ km per generation, in $minimax=[9.3, 24.6]$. Using whole zone estimate of~~
651 ~~density provided $\delta_{Maro}=19.2$ km per generation in $minimax=[10.8, Infinity]$, where infinity~~
652 ~~probably means the maximum distance observed between two traps $\delta_{max}=32.5$ km.~~

653

654 Population genetics structure regarding reproduction of tsetse flies from Dokoutou and 655 Timbéri and Dokoutou

656 After correction for stuttering at loci Gff8, 12 and Gff18 (Appendix 3), there was still
657 a small but not significant heterozygote deficit ($F_{IS}=0.031$, in $95\%CI=[-0.045, 0.144]$, p -
658 value=0.2906) (panmictic populations), with some evidence of rare null alleles at some loci
659 but with a complete disconnection with the too rare missing genotypes frequencies. We
660 thus chose not to recode these missing genotypes for FreeNA computations.

661

Mis en forme : Police :Italique

Mis en forme : Police :Italique

Mis en forme : Retrait : Gauche : 0 cm, Suspendu : 1,25 cm

662 *Global subdivision between Dokoutou and Timbéri*

663 Subdivision between the two zones was highly significant ($F_{ST}=0.08$ in
664 $95\%CI=[0.055, 0.101]$, $p\text{-value}<0.0001$). Corrected F_{ST} was a little smaller
665 ($F_{ST_FreeNA}=0.0745$ in $95\%CI=[0.05, 0.0938]$). The correlation between G_{ST} and H_S was
666 positive. We thus used $H_S=0.651$, and $H_T=0.679$ to compute $G_{ST}=0.227$. Interestingly,
667 recoded $F_{ST_FreeNA\text{-max}}=0.3274$ provided the same value for $F_{ST_FreeNA}'=0.2276$ in
668 $95\%CI=[0.154, 0.2864]$ as for G_{ST} . We thus chose Meirmans' method, to keep 95% CIs.
669 This allowed the computation of an effective number of immigrants $N_e m=0.4$ in
670 $95\%CI=[0.3, 0.7]$ individuals per generation (with two subpopulations), exchanged
671 between the two zones (e.g. ~ one individual every six months).

672
673 *Isolation by distance within and between Dokoutou and Timbéri*

674 Isolation by distance was explored first using traps as subsample units, with F_{ST} -
675 $FreeNA$, but without recoding missing data, as these did not correspond to actual null
676 homozygotes. With all traps of the two foci, isolation by distance was significant with a
677 slope $b_{DT\text{-traps}}=0.0144$ in $95\%CI=[0.001, 0.0208]$, a neighborhood size $N_b=69$ individuals in
678 $95\%CI=[48, 1031]$, and an effective number of immigrants from neighboring traps $N_e m=11$
679 individuals per generation in $95\%CI=[8, 164]$.

680 Within each site (separately), isolation by distance between traps provided a
681 negative slope in Dokoutou for the average and the $95\%CI$, and f. For Timbéri, only the
682 upper limit was positive ($b_{Timbéri\text{-Traps-u}}=0.033$), with a corresponding lower $N_b=30$
683 individuals and $N_e m=5$ individuals per generation. However, the low number of traps and
684 the existence of traps with a single (unusable) fly led us to test isolation by distance
685 between traps with a D_{CSE} based Mantel test. The result was significant (one sided p -
686 value=0.0019). Isolation by distance between individuals, using parameter \hat{e} , gave similar
687 results in Dokoutou (all slopes were negative), and Timbéri (only the upper limit was
688 positive, $b_{Timbéri\text{-Ind-u}}=0.0044$). For Timbéri, the corresponding lower $N_b=226$ individuals
689 and $N_e m=36$ individuals per generation. Using subsites, we observed a significant
690 isolation by distance in Timbéri with $b_{Timbéri\text{-subsites}}=0.0095$ in $95\%CI=[0.0042, 0.0147]$,
691 $N_b=105$ in $95\%CI=[69, 238]$, $N_e m=17$ in $95\%CI=[11, 38]$.

692
693 *Effective population size of Dokoutou and Timbéri*

694 We could not get many usable values for N_e , especially for Dokoutou, which only
695 provided infinite results, except with Balloux's method. Nevertheless, we used the rare
696 cases where a lower limit of $95\%CI$ was available were used as a lower limits to N_e in that

Mis en forme : Paragraphes solidaires

Mis en forme : Police :Italique

Mis en forme : Police :Italique

Mis en forme : Police :Italique

697 zone. These lower limits all suggested higher values in Dokoutou than in Timbéri (Table
698 3). We used these lowest values to obtain "minimum" averages of effective population
699 densities. Doing so, actually considerably extended the range of possible N_e 's in both
700 zones.
701 Over the two zones, average $N_e=38$ in minimax=[6, 105]. Nevertheless, a
702 As the two
703 zones are quite isolated from each other, the total (combined) effective population size can
704 be assumed to correspond to the sum of the effective population sizes in each Dokoutou
705 and Timbéri. Hence $N_{e-Tot}=76$ in minimax=[12, 209].

Effective population densities in Dokoutou and Timbéri

706 As seen above, surfaces of these two zones were 0.2452 and 1.37 km² for
707 Dokoutou and Timbéri respectively. Timbéri displayed an important effective population
708 density $D_e=20$ individuals/km² in minimax=[0, 67], while Dokoutou appeared as extremely
709 dense with more than 200 individuals/km² in minimax=[49, 478] (Table 3). Over the two
710 zones, $N_e=38$ in minimax=[6, 105]. Using the number of immigrants computed above, the
711 immigration rate was $m=0.0111$ on average, and varied between 0.0029 and 0.1132
712 (minimum and maximum values). The average distance between traps of the two foci was
713 $D_{Timbéri-Dokoutou}=50$ km. We could thus estimate a rough proxy for the average dispersal
714 distance ($m \times D_{Timbéri-Dokoutou}$) $\delta_{TD}=557$ m per generation, with a variation between 149 and
715 5662 meters, which looked much smaller than what was observed in the other two zones
716 (Mandoul and Maro).
717

Mis en forme : Police :Italique

719 Table 3: Effective population sizes (N_e) of *Glossina fuscipes fuscipes* in Dokoutou and
 720 Timbéri (Chad), with different methods, and 95%CI (between brackets) when
 721 available, and averaged across methods; and minimum and maximum values
 722 observed. The surface (S) of Timbéri, in km², was computed with geosphere for R
 723 and as described in the Material and Methods section for Dokoutou. Averaged
 724 values of N_e were used to compute effective population densities (D_e) with N_e/S and
 725 minimum and maximum values observed across methods. The lowest value of 95%
 726 confidence intervals was used to compute averages when nothing else was
 727 available.

		Focus	
		Dokoutou	Timbéri
N_e	Method		
	LD	Infinite [117.3, Infinite]	92 [23, Infinite]
	Coancestry	Infinite	13 [6, 22]
	Estim	Infinite [18, Infinite]	Infinite [0, Infinite]
	Balloux	12	4
	Average	49 [12, 117]	27 [0, 92]
S (km ²)		0.2453	1.3712
D_e (individuals/km ²)		200 [49, 478]	20 [0, 67]

728
 729 ~~Isolation by distance was explored first using traps as subsample units, with F_{ST-}~~
 730 ~~$F_{ST-FreeNA}$, but without recoding missing data. With all traps of the two foci, isolation by distance~~
 731 ~~was significant with a slope $b_{TD-traps}=0.0144$ in 95%CI=[0.001, 0.0208], a neighborhood~~
 732 ~~size $N_b=69$ individuals in 95%CI=[48, 1031], and an effective number of immigrants from~~
 733 ~~neighboring traps $N_e m=11$ individuals per generation in 95%CI=[8, 164].~~
 734 ~~As the two zones are quite isolated from each other, the total effective population~~
 735 ~~size can be assumed to correspond to the sum of the effective population sizes in each.~~
 736 ~~Hence $N_e-Total=76$ in minimax=[12, 200]. Considering that the space between Timbéri and~~
 737 ~~Dokoutou was empty (which seemed accurate),~~
 738 ~~The total surface occupied by all traps of both foci was $S_{TD-SDT_Area}=3392662$ m²~~
 739 ~~(computed with the `areaPolygon` function). This led to an effective population density~~
 740 ~~$D_{e_TD-trapsDTI}=22$ individuals/km² in minimax=[4, 62], and an estimate of dispersal δ_{TD-}~~
 741 ~~$traps=993$ m per generation in 95%CI=[826, 3824] and minimax=[498, 9580], which~~
 742 ~~appeared very close to the $F_{ST-FreeNA}$ -based estimation given above. Within each site~~
 743 ~~(separately), isolation by distance between traps provided a negative slope in Dokoutou for~~
 744 ~~the average and the 95%CI, and for Timbéri only the upper limit was positive ($b_{Timbéri-}$~~

Mis en forme : Police :Italique

$u=0.033$), with a corresponding lower $N_b=30$ individuals and $N_e m=5$ individuals per generation. For Timbéri, $D_e=20$ individuals/km² in minimax=[0, 67], which would give $\delta_{Timbéri-Traps}=699$ m/generation in minimax=[13, infinity], where infinity may correspond to the maximum distance between two traps (4876 m). This is also in the range estimated before, though this average represents only a 7th of the width of this (almost) panmictic site. However, the low number of traps and the existence of traps with a single (unusable) fly led us to test isolation by distance between traps with a D_{GSE} -based Mantel test. The result was significant (one-sided p value=0.0049). Isolation by distance between individuals, using parameter δ , gave similar results in Dokoutou (all slopes were negative), and Timbéri (only the upper limit was positive, $b_{Timbéri-u}=0.0044$). For Timbéri, the corresponding lower $N_b=226$ individuals and $N_e m=36$ individuals per generation and $\delta_{Timbéri-Traps}=1000$ m/generation in minimax=[5, infinity]. These values lied again into the window of values computed above. Isolation by distance between subsites was only possible in Timbéri. It gave a significant result with $b_{Timbéri-subsites}=0.0095$ in 95%CI=[0.0042, 0.0147], $N_b=105$ in 95%CI=[69, 238], $N_e m=17$ in 95%CI=[11, 38], and $\delta_{Timbéri-subsites}=1304$ m per generation in 95%CI=[1048, 1961] with a minimax=[568, infinity]. These values were not significantly different from those measured between traps across the two zones (as can be seen above). Hence, whatever the scale of study, F_{ST} -based between the two populations, isolation by distance over all or within Timbéri alone, or between individuals, dispersal distance was almost the same: $\delta_{average}=1002$ m/generation in minimax=[247, 5974].

Mis en forme : Police :Italique

Dispersal distances within and between Dokoutou and Timbéri

Using the number of immigrants between Dokoutou and Timbéri and averaged N_e computed above, the immigration rate was $m=0.0111$ on average, and varied between 0.0029 and 0.1132 (minimum and maximum values). The average distance between traps of the two foci was $D_{DT}=50$ km. We could thus estimate a rough proxy for the average dispersal distance ($m \times D_{DT}$) $\delta_m=557$ m per generation, with a variation between 149 and 5662 meters, which looked much smaller than what was observed in the other two zones (Mandoul and Maro).

Between traps, over both zones, we computed an estimate of dispersal δ_b . All=993 m per generation in 95%CI=[826, 3824] and minimax=[498, 9580], which appeared very close to δ_m .

In Timbéri, still between traps, δ_b within=699 m/generation in minimax=[13, infinity], where infinity may correspond to the maximum distance between two traps in that zone

Mis en forme : Police :Italique

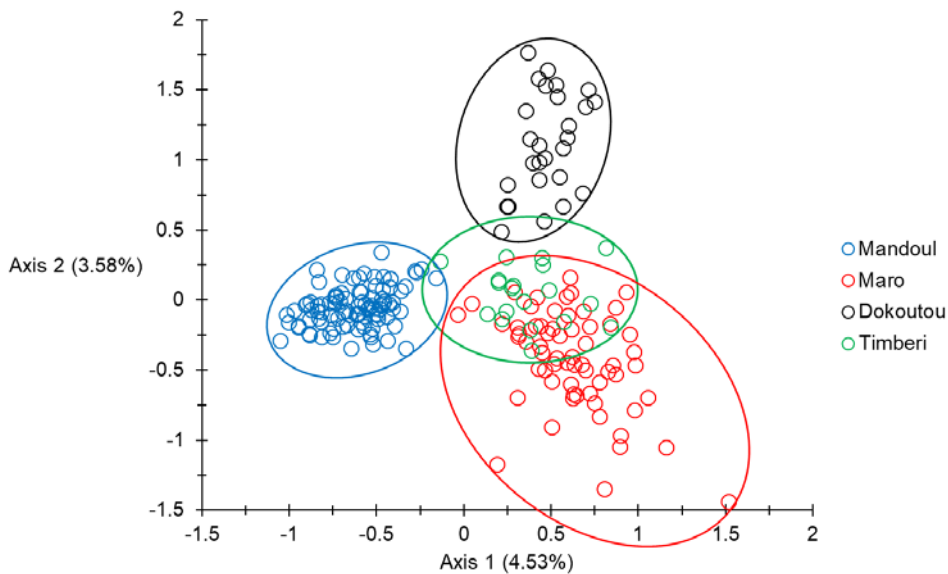
(i.e. 4876 m). This is also in the range estimated before. ~~and~~ Still in Timbéri, but between individuals. $\bar{\delta}_{\text{Timbéri-Traps-Individuals}}=1909$ m/generation in $\text{minimax}=[5, \text{infinity}]$. These values lied again into the window of values computed above. ~~Finally,~~ isolation by distance between subsites was only possible in Timbéri, and $\bar{\delta}_{\text{Timbéri-subsites}}=1304$ m per generation in $95\%CI=[1048, 1961]$ with a $\text{minimax}=[568, \text{infinity}]$.

All ~~t~~ These values were not significantly different from ~~those measured between traps across the two zones (as can be seen above)~~ ~~each others~~. Hence, whatever the scale of study, F_{ST} based between the two populations, isolation by distance over all or within Timbéri alone, ~~or between subsites, traps or individuals,~~ dispersal distance was almost the same: $\bar{\delta}_{\text{average}} \approx 1092$ m/generation in $\text{minimax} \approx [247, 5974]$.

Factorial components analysis (FCA), DAPC and NJTRee analyses

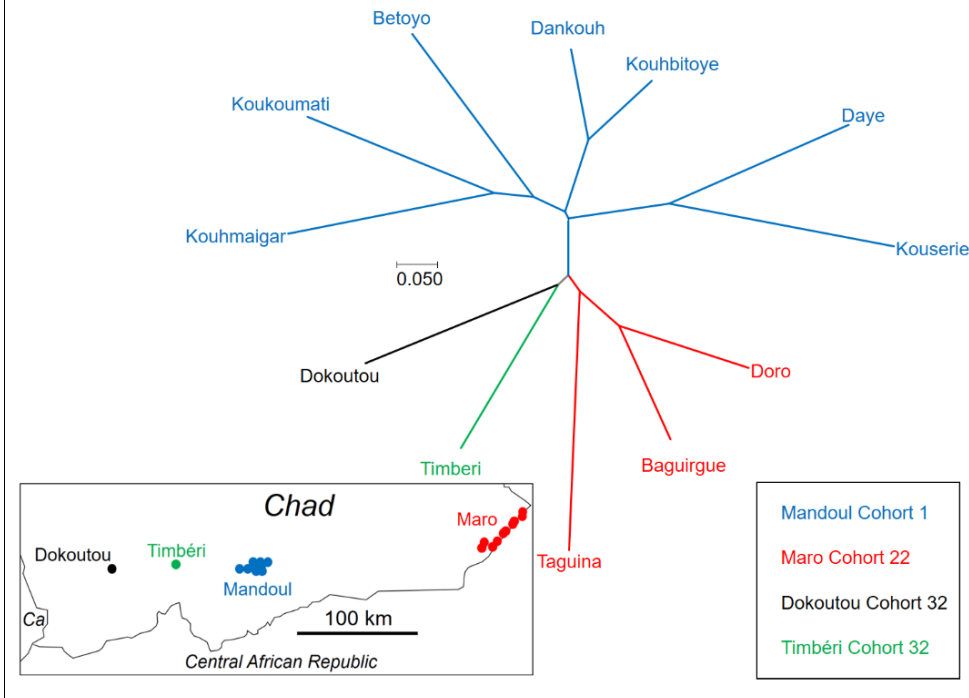
The results of the FCA analysis is presented in Figure 2. The two first axes were significant according to the broken stick criterion (highest expected percentages of inertia $I_{E1}=3.77$, and $I_{E2}=3.09$; observed ones $I_{O1}=4.53$ and $I_{O2}=3.38$ respectively). Axis 1 separated rather well Mandoul individuals from individuals from other samples, except for a few individuals that seemed close to Timbéri or Maro. The second axis separated Dokoutou, except for a few individuals that appeared close to individuals from Timbéri or Maro. Most other flies from Timbéri seemed to belong to the same pool defined by Maro individuals. Maro appeared very heterogeneous, which suggested substantial immigration from nearby (genetically close) or even remote (genetically distant) sites. Some outliers also suggested recruitment of flies from zones that were not sampled. It is difficult to clearly see the contribution of spatial and temporal distances to that picture. Spatially, Maro appeared as the most remote zone, while temporally, Mandoul is by far the most isolated one.

807 Figure 2: Presentation of the two dimensions projection of individuals of *Glossina fuscipes*
 808 *fuscipes* from different zones (with different colors) from Southern Chad according
 809 to the first two axes of a Factorial correspondence analysis. Percent of inertia are
 810 indicated. Both Axes 1 and 2 were significant. Mandoul flies belong to cohort 1,
 811 Maro to cohort 22 and Dokoutou and Timbéri to cohort 32.



812
 813
 814 The DAPC analysis offered a very confused picture that was impossible to interpret
 815 biologically. This analysis is presented and discussed in Appendix 4.
 816 The NJTree brought some more light (Figure 3) as temporal distances apparently
 817 affected more the distribution of branch lengths than geographic distances. Indeed, Maro
 818 and Dokoutou, which were the two most remote zones, were relatively close in the tree
 819 and only 10 generations apart, while Mandoul sites, which were geographically closer to
 820 Timbéri, but temporally very distant (31 generations), appeared as the most remote
 821 lineage of the tree. This was confirmed by the partial Mantel test that provided a higher
 822 partial correlation of D_{CSE} with temporal distances ($r_{Temporal}=0.3175$, $p\text{-value}<0.0001$) than
 823 with geographic distances ($r_{Geographic}=0.2108$, $p\text{-value}=0.0041$).
 824

825 Figure 3: Neighbor-joining Tree based on Cavalli-Sforza and Edward's chord distance
 826 between the different sites of Southern Chad for *Glossina fuscipes fuscipes*. Zones
 827 and cohorts are indicated with the same colors as for Figures 2.



828

829

830

831 *Sex specific genetic structure*

832 Subsamples with only one gender or one individual were removed for these
 833 analyses to avoid error messages. Measures were contradictory depending on the statistic
 834 or the cohort used (Table 4). Globally, no test was significant (p -values>0.19), even if
 835 there was some tendencies toward male biased dispersal.

836

837 Table 4: Results of the sex specific genetic structure analyses undertaken in the different
 838 cohorts available, for the different statistics used. Significance (p -values) and their
 839 combination with the generalized binomial procedure (All) are also given. All tests
 840 were one-sided (alternative hypothesis H1: males disperse more). Values indicating
 841 the "most dispersive gender" are in bold. C1: Mandoul; C22: Maro; and C32:
 842 Dokoutou-Timbéri. Note that with three tests, the maximum possible combined p -
 843 value (All) was 0.125.

Parameter tested	C1	C22	C32	All
mA_{Ic} Females	0.1862	0.1100	-0.3838	-0.0282
Males	-0.4276	-0.2781	0.3838	-0.1073
p -value	0.1672	0.2925	0.8069	>0.1250
vA_{Ic} Females	5.6234	6.5356	11.2584	7.8058
Males	8.6431	5.9403	5.5601	6.7145
p -value	0.0932	0.4934	0.9363	>0.1250
F_{ST} Females	0.0095	-0.0106	0.0792	0.0260
Males	0.0056	-0.0275	0.0655	0.0145
p -value	0.4971	0.3219	0.3081	0.1229

844

845

846 *Bottleneck detection*

847 For these analyses, following the previous results, we considered Mandoul, Maro,
 848 Dokoutou, and Timbéri as four different subpopulations. The results of these analyses are
 849 presented in Table 5. Globally, we found a rather convincing evidence of a bottleneck
 850 signature. Locally, only Mandoul and Timbéri presented a moderately and a strongly
 851 (respectively) significant signature of bottleneck.

852

853 Table 5: Results of the Bottleneck analysis for different samples, and for different models
 854 of mutations (IAM, TPM, and SMM). For each model of mutation, p -values were
 855 combined with the generalized binomial test (All), with the adapted optimal number
 856 of tests considered ($k=2$), following rules defined for this procedure (see text).

Sample	IAM	TPM	SMM
Mandoul	0.0019	0.0644	0.1797
Maro	0.9356	0.9932	1
Dokoutou	0.1016	0.5898	0.999
Timbéri	0.001	0.0049	0.4102
All	<0.0001	0.0228	0.5425

857

858

859 Discussion

860 Although null alleles explained most heterozygote deficits, there was a tendency for
 861 stuttering at several loci. Stuttering was quite variable across the different zones: no
 862 evidence in Mandoul, five loci were probably affected in Maro, and three loci in Dokoutou
 863 and Timbéri. Fortunately, no SAD was evidenced in any of these samples. Stuttering and
 864 null alleles issues were taken care of before further analyses and inferences were made.
 865 Nevertheless, finding a way to avoid more efficiently amplification problems remains a
 866 progress that would be very welcome for the study of tsetse flies.

867 The strongly female biased sex-ratio observed in the least dense zones is difficult to
 868 understand. As can be seen in Table 6, densities of trapped flies were strongly correlated
 869 with effective population densities ($\rho=1$, p -value=0.0417, one-sided), which gives some
 870 reliability to density estimates and its correlation with SR . The data suggested that
 871 populations with very low densities contain much more females than males, whereas the
 872 sex ratio becomes more balanced in areas with higher population densities. It might also
 873 be that males from low-density populations respond less to biconical traps than females, a
 874 phenomenon that would tend to disappear in the sites with higher population densities
 875 (Table 6). Sites with high tsetse population densities may correlate with higher resource
 876 availability (more hosts) where females, with higher energy requirements, do not need to
 877 fly a lot to find a host for feeding. Alternatively, females need to spend more time flying in
 878 zones with scattered hosts on which to feed, and hence, would be more easily trapped,
 879 while male with smaller energy needs would fly less and not be so much exposed to
 880 trapping signals as females. Another non-exclusive hypothesis would relate to the density
 881 of suitable spots for larviposition. Pregnant females are known to be highly selective

882 before choosing a site where to larviposit (Gimonneau et al., 2021). In zones with higher
 883 densities of suitable larviposition spots, females do not need to search far away for
 884 larvipositing their larva, while in zones with less suitable larviposition spots, females would
 885 spend more time searching for suitable sites and hence, have a higher probability of being
 886 captured in biconical traps. Males can mate with virgin females that emerge from pupae in
 887 the larviposition sites soon after their imaginal molt, or when feeding on a host. This is
 888 however unlikely to influence trap catches, as tsetse responses to traps are feeding
 889 responses and not mating responses. If density negatively correlates with female dispersal
 890 distances, our observations may also be related to other disturbing results (De Meeûs et
 891 al., 2019). Although the above may seem highly speculative, it opens new routes for
 892 specific field and experimental investigations to better understand the density-dependent
 893 effects on the ecology of tsetse flies.

894

895 Table 6: Synthesis of numbers and densities of *Glossina fuscipes fuscipes* captured in
 896 traps (N_t and D_t), of effective population sizes and densities (N_e and D_e), and of
 897 Sex-ratio in the different zones of Southern Chad.

	Mandoul	Maro	Dokoutou	Timbéri
S (km ²)	32	227	0.2	1.4
N_t	148	67	27	22
N_e	141	28	49	27
D_t (/km ²)	4.6	0.3	49.1	16
D_e (/km ²)	4.4	0.1	110.1	20
Sex ratio	0.51	0.37	1.25	0.83

898

899 Effective population densities in the Mandoul and Maro sites, which are active HAT
 900 foci, were similar to those at the lower limit found in the tsetse literature (De Meeûs et al.,
 901 2019) (Table 6). In those sites, the convergence between effective population densities
 902 and density of trapped flies was high, with $D_e < D_t$ for the smallest values, and the reverse
 903 for the highest ones. This may be due to the fact that the proportion of trapped flies as
 904 compared with the real population size decreased as the density increased. If this was
 905 true, the fly density in Dokoutou and Timbéri, the sites with the highest fly density and
 906 where $D_e > D_t$, should have maintained many tsetse flies after the first sampling campaign.
 907 Only a second future sampling campaign could test this prediction.

908 At the scale of each different site, dispersal distances were among the highest
 909 recorded for tsetse flies (De Meeûs et al., 2019), in particular for the Mandoul and Maro

910 sites, where an almost free movement across the whole range within each of these foci
911 was apparent, i.e. 24 km and 32 km, respectively. In Dokoutou, only 213 m wide, or
912 Timbéri, 5 km wide, effective dispersal distances were as large as, or larger than the size
913 of these areas. Dokoutou and Timbéri were separated by an average distance of 50 km,
914 but a genetic signature of a moderate exchange of immigrants was obvious between the
915 two sites: i.e. between one to two individuals every three generations (i.e. six months). We
916 observed a tight convergence of dispersal distances estimated from the F_{ST} computed
917 either between the two zones, or from isolation by distance between traps between the two
918 zones, or between individuals, traps or subsites in Timbéri alone. This brings confidence to
919 these estimates. In the literature, a maximum dispersal distance of 25 km in 24 days was
920 reported during a mark-release-recapture study with a wild female *Glossina tachinoides*
921 (Cuisance et al., 1985). Twenty-four days is less than half a generation. This distance was
922 covered in riparian forest bordering a river and not across rivers. Nevertheless, the riverine
923 tsetse species *Glossina palpalis gambiensis* has shown to be able to cross watersheds
924 between different river basins, even when the habitat was less favourable (Vreysen et al.,
925 2013). Although it might be a rare event, covering such a distance between Dokoutou and
926 Timbéri rivers in three generations should not be totally ruled out, especially during
927 favorable periods (rainy season), and using indirect trajectories, in particular via the
928 Southern and more favorable part of the country. Alternatively, we can use equation 9.13a
929 (p 502) of (Hedrick, 2005a) to explain the moderate genetic divergence observed between
930 Dokoutou and Timberi, in absence of any gene flow, i.e. $g = -2N_e \ln(1 - G_{ST})$, where g is the
931 number of tsetse generations, N_e is the average effective population size across the two
932 zones, and G_{ST} is the standardized F_{ST} estimate of Meirmans and Hedrick (Meirmans &
933 Hedrick, 2011). In that case, the two zones were completely isolated from each other only
934 3.3 years before sampling in $\text{minimax} = [0.5, 9]$, for a two-months generation time (4.9 in
935 $\text{minimax} = [0.8, 13]$ for three months generation time). Although this is theoretically
936 possible, such an abrupt and very recent environmental split is quite hard to envision. The
937 Mandoul control campaign, including the exploration of the surroundings, took place in
938 November 2013, i.e. five years before the sampling in Dokoutou-Timbéri, and there is no
939 evidence of an environmental continuity between Timbéri and Dokoutou that was followed
940 by an abrupt interruption. In addition, historical imagery of Google Earth Pro also does not
941 show any evidence of such an abrupt split in land cover between 2012 and 2018
942 (Supplementary File S2). Instead, the vegetation gap between the two zones was already
943 visible in 2013, and a very progressive and slow decline of "green areas" is obvious
944 between 2013 and 2018, with an apparent very slight acceleration in 2017. Moreover, if so,

945 it is hard to understand the convergence of dispersal distances estimates using different
946 models, between Dokoutou and Timbéri, or within Timbéri alone. Rare gene exchanges
947 (between one and two alleles every six months) between spots separated by 50 km of
948 unsuitable landscapes as the crow flies, even if questionable, seems a reasonable
949 interpretation of our population genetics results.

950 Very rare gene exchange may also hold for Mandoul and the CAR border (40 km),
951 with several river courses in between. This was also suggested by the FCA analysis,
952 where some individuals (or part of their genetic inheritance) may have been exchanged
953 between the different zones. Such migration events would be extremely hard to observe,
954 unless people deploy prohibitively large, intense and perennial trapping campaigns
955 between the different zones investigated. On the other hand, the rarity of such an incident,
956 renders the probability of reinvasion of eradicated zones very unlikely, since it would need
957 the immigration of one fertilized female or one female and one male, at least.

958 Trypanosome prevalence in humans was estimated as $P \approx 0.02$ before the control begun in
959 Mandoul and Maro, and around 6% of tsetse flies were found positive for *T brucei* sp
960 (Ibrahim et al., 2021). If we consider that trypanosome prevalence could reach values
961 much lower than that as a result of medical and entomological campaigns, the probability
962 of reinvasion with infected tsetse can reasonably be estimated as null.

963 The south border with Central African Republic (CAR) is located close to Maro and
964 has not been investigated entomologically. It may represent many potential unexplored,
965 and possibly tsetse rich environments and thus potential sources for reinvasion with tsetse
966 flies. This may explain the great genetic heterogeneity of tsetse flies from Maro, and this
967 focus will therefore need special attention.

968 Significant male-biased dispersal has rarely been found in tsetse flies, i.e. once with
969 *G. palpalis* in Cameroon (Mélachio et al., 2011), and twice with *G. tachinoides* in Burkina
970 Faso (Kone et al., 2011; Ravel et al., 2013). Nevertheless, the lack of such research in the
971 literature makes it difficult to draw any solid conclusion whether male tsetse flies disperse
972 more than females. Although there was a tendency with *G. f. fuscipes* from Chad, it was
973 not significant. If females tend to disperse less, they may be less available to trapping
974 devices. The higher proportions of females found in traps, at least in Mandoul and Maro
975 (the least dense zones), were not in line with this interpretation. Mark-release studies have
976 found evidence for female-biased dispersal in some instances (Hargrove & Vale, 1979;
977 Vale et al., 1984; Vreysen et al., 2013), but this is in contrast with the almost absence of
978 genetic signatures. Again, this would require further specific investigations to be fully

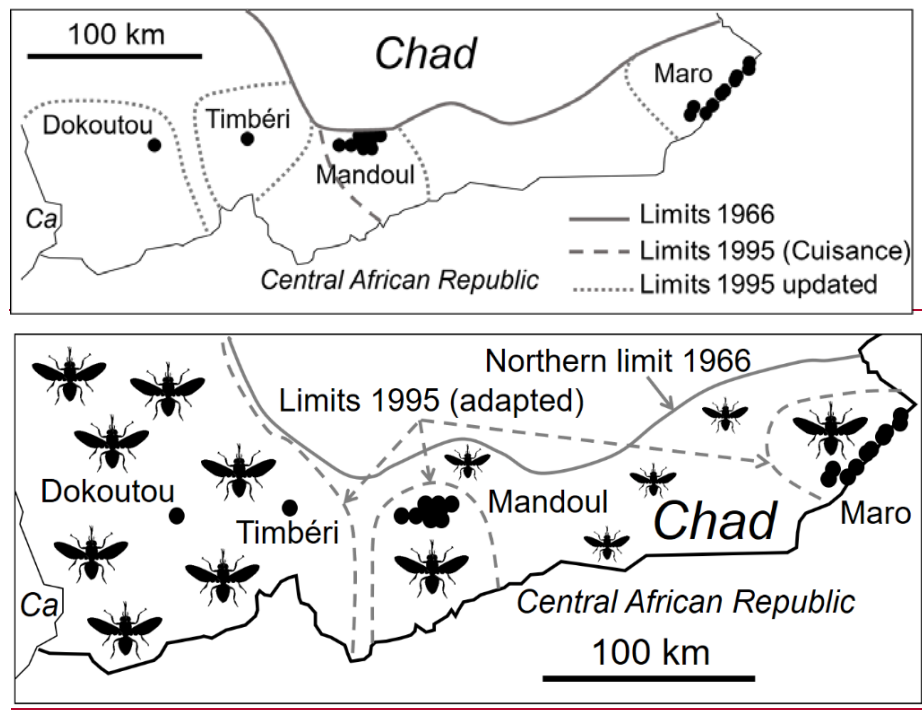
979 understood, but whether females disperse more or less than males may be relevant for
980 control programs.

981 A moderate and strong bottleneck signature was found in Mandoul and Timbéri,
982 respectively. Previous reports have indicated the geographical retraction of the distribution
983 of tsetse flies in southern Chad (Gruvel, 1966; Cuisance, 1995) mainly due to periods of
984 drought and human activities that have dramatically reduced and fragmented suitable and
985 interconnected habitats into small and isolated subpopulations of tsetse flies around the
986 1990s. For some reasons, the signature of such events would have been kept in Mandoul
987 and Timbéri but not in Maro or Dokoutou. For Maro, frequent immigration from southern
988 tsetse fly populations may easily have removed any bottleneck signature and Dokoutou
989 was probably too small a sample to detect any bottleneck signature (type error 2). The
990 extreme high population density found in that zone may also have limited the effect of such
991 isolation.

992 We may use Cornuet and Luickart's (Cornuet & Luikart, 1996) model as explained
993 above and in an earlier paper (De Meeüs et al., 2010) to extrapolate some informative
994 parameters. With 9 loci, subsample sizes of 96 for Mandoul and 19 for Timbéri, and
995 genetic diversity $H_S=0.643$ and 0.659 , respectively, the detection of a bottleneck would
996 have been possible with various scenarios. Nevertheless, given the actual population sizes
997 currently observed in the two populations, it seems that the most likely combination of
998 parameters for both zones and both models (IAM and TPM) may have been $\tau=1$ and
999 $\alpha=1000$ (i.e. a drastic bottleneck). If so, with 108 and 138 generations since 1995 for
1000 Mandoul and Timbéri, respectively, these parameter combinations lead to $N_{e\text{-post}}=54$ for
1001 Mandoul, and $N_{e\text{-post}}=69$ for Timbéri, for the effective population sizes after the bottleneck.
1002 These values correspond to the range of values of N_e we computed for these two zones.
1003 We also computed $N_{e\text{-pre}}=54000$ according to Mandoul parameters, and $N_{e\text{-pre}}=69000$ for
1004 Timbéri, before the bottleneck. Such values, if they corresponded to anything, would
1005 probably match the global and interconnected big populations that inhabited the area
1006 before 1995. This seems to match for Mandoul, and hence Maro, that appeared as
1007 probable isolated pockets in 1995 (Figure 4). However, in 1995, Timbéri and Dokoutou
1008 were still apparently connected (Figure 4). So maybe the fragmentation occurred later
1009 between these two zones, or the 1995 investigations were not accurate enough at that
1010 time to detect a hiatus between Dokoutou and Timbéri. No matter the real scenario,
1011 populations of *G. fuscipes fuscipes* seem to have strongly declined from very high
1012 population densities to the very low densities observed during this work, at least in
1013 Mandoul and to a lesser extent in Maro.

1014
1015
1016
1017
1018
1019
1020

Figure 4: Map of sample locations (dots) of *Glossina fuscipes fuscipes* of the present study with the Northern limit described by Gruvels of distributions of the species in 1966 (Gruvel, 1966) (grey line, small and big shadow flies), and speculated limits in 1995 (grey dashed lines, big shadow flies), combining different surveys: ancient (Cuisance, 1995) and more recent adapted according to recent surveys (Signaboubo et al., 2021), including the present one. (Ca: Cameroon).



1021
1022
1023
1024
1025
1026
1027
1028
1029
1030
1031
1032

Conclusion

Population genetics confirmed the field observations of a strong subdivision between tsetse populations in Southern Chad, together with very low population densities. Therefore, the probability of reinvasion from neighboring zones are (very) small, at least in Mandoul, Timbéri and Dokoutou. In addition, efficient barriers might be deployed permanently to prevent reinvasion from the southern areas. This was particularly obvious for the Maro focus that appeared to present the higher reinvasion risks. Tsetse eradication may thus be considered as a sustainable option for HAT elimination in Mandoul focus.

1033 ~~Control can also be advised in the Dokoutou-Timbéri zone where HAT has not been~~
1034 ~~reported yet but where AAT may cause problems on animal Health.~~ For the Maro HAT
1035 focus, another strategy based on continuous tsetse suppression will probably be needed.
1036

1037 **Acknowledgements**

1038 This study was financed by the International Atomic Energy Agency (IAEA), Austria.
1039 The authors thank Giuliano Cecchi (FAO) for providing hydrographic base maps of
1040 Southern Chad ~~and two anonymous referees whose suggestions and remarks helped to~~
1041 ~~considerably improve the present manuscript.~~ Authors would like to dedicate this paper to
1042 our colleague and friend Dr Jean-Baptiste Rayaisse (1967–2020). Jean-Baptiste was a
1043 hard worker, very efficient researcher, deeply committed to trypanosomosis control, and
1044 with a great sense of humour. All the community misses him immensely. ~~We will also miss~~
1045 ~~Pèka Mallaye, who passed away the 13/08/2022, who was of great help as the coordinator~~
1046 ~~of the Chadian PNLTHA.~~
1047

1048 **Author's contributions**

1049 All authors read, amended and/or approved the final manuscript, except JBR who could
1050 not check the last versions.

1051 Conceptualization: Mallaye Peka, Jean-Baptiste Rayaisse, Adrien Marie Gaston Belem,
1052 Philippe Solano, Jérémy Bouyer, Camille Noûs.

1053 Sampling and field work: Mahamat Hissene Mahamat, Mallaye Peka, Jean-Baptiste
1054 Rayaisse, Mahamat, Justin Darnas, Brahim Guihini Mollo, Wilfrid Yoni, Jérémy
1055 Bouyer, Rafael Argiles-Herrero.

1056 Genotyping, genotype interpretation and corrections: Sophie Ravel, Adeline Ségard.

1057 Data analyses: Thierry de Meeûs.

1058 Maps and design of figures: Jérémy Bouyer and Thierry de Meeûs.

1059 Writing of the original draft: Sophie Ravel, Thierry de Meeûs.

1060 Supervision: Mallaye Peka, Jean-Baptiste Rayaisse, Philippe Solano, Thierry de Meeûs,
1061 Sophie Ravel.
1062

1063 **Data availability**

1064 Raw data are available in supplementary file S1 "Gff-TchadDataSupFile1.xlsx".

1065 Position of traps, dates of sampling and cohort of flies are available in the supplementary
1066 Figure S1 "GffChadCaptureMapsFigS1.tif". Land cover images from Google Earth Pro
1067 between Timbéri and Dokoutou for the years 2012-2018 are presented in the

1068 supplementary file "DokTimb2012-2018GoogleEarthSupFileS2.pptx ". Example of scripts
1069 to compute geographic distances and surfaces with the package geosphere is available in
1070 Appendix 1. HierFstat scripts and results are available in the Appendix 2. Detailed
1071 analyses of quality testing of data are in Appendix 3 .Data for the DAPC analysis (package
1072 adegenet) are in the file "GffChadSpatialTrapsDAPC.txt", and the corresponding script and
1073 results in Appendix 4.

1074

1075 **Conflict of interest disclosure**

1076 The authors declare that they have no financial conflict of interest with the
1077 content of this article. Philippe Solano and Adrien Marie Gaston Belem are
1078 recommenders of PCI Infections. Thierry de Meeûs is one of the PCI Infections
1079 administrators.

1080

1081 **References**

1082 Balloux, F. (2004) Heterozygote excess in small populations and the heterozygote-excess
1083 effective population size. *Evolution*, **58**, 1891-1900.

1084 Belkhir, K., Borsa, P., Chikhi, L., Raufaste, N., Bonhomme, F. (2004) GENETIX 4.05,
1085 logiciel sous Windows TM pour la génétique des populations. Laboratoire Génome,
1086 Populations, Interactions, CNRS UMR 5000, Université de Montpellier II, Montpellier
1087 (France).

1088 Benjamini, Y., Yekutieli, D. (2001) The control of the false discovery rate in multiple testing
1089 under dependency. *The Annals of Statistics*, **29**, 1165–1188.

1090 Bouyer, J., Desquesnes, M., Yoni, W., Chamisa, A., Guerrini, L. (2015) Attracting and
1091 trapping insect vectors, Technical guide GeosAf, 2. s.n., s.l., France, p. 23.

1092 Bouyer, J., Solano, P., de la Rocque, S., Desquesnes, M., Cuisance, D., Itard, J., Frézil,
1093 J.-L., Authié, É. (2009) Trypanosomoses: control methods, in: Lefèvre, P.C., Blancou, J.,
1094 Chermette, R., Uilenberg, G. (Eds.), *Infectious and Parasitic Diseases of Livestock*.

1095 Lavoisier (Tec & Doc), Paris, pp. 1936–1943.

Mis en forme : Français (France)

1096 Brookfield, J.F.Y. (1996) A simple new method for estimating null allele frequency from
1097 heterozygote deficiency. *Molecular Ecology*, **5**, 453-455.

1098 Büscher, P., Bart, J.M., Boelaert, M., Bucheton, B., Cecchi, G., Chitnis, N., Courtin, D.,
1099 Figueiredo, L.M., Franco, J.R., Grébaud, P., Hasker, E., Ilboudo, H., Jamonneau, V., Koffi,
1100 M., Lejon, V., MacLeod, A., Masumu, J., Matovu, E., Mattioli, R., Noyes, H., Picado, A.,
1101 Rock, K.S., Rotureau, B., Simo, G., Thévenon, S., Trindade, S., Truc, P., Van Reet, N.
1102 (2018) Do cryptic reservoirs threaten gambiense-sleeping sickness elimination? *Trends in*
1103 *Parasitology*, **34**, 197-207. 10.1016/j.pt.2017.11.008

1104 Cavalli-Sforza, L.L., Edwards, A.W.F. (1967) Phylogenetic analysis: model and estimation
1105 procedures. *American Journal of Human Genetics*, **19**, 233-257.

1106 Challier, A., Laveissière, C. (1973) Un nouveau piège pour la capture des glossines
1107 (*Glossina*: Diptera, Muscidae): description et essais sur le terrain. *Cahier de l'ORSTOM*,
1108 *Série Entomologie Médicale et Parasitologie*, **11**, 251-262.

1109 Chapuis, M.P., Estoup, A. (2007) Microsatellite null alleles and estimation of population
1110 differentiation. *Molecular Biology and Evolution*, **24**, 621-631. 10.1093/molbev/msl191

1111 Coombs, J.A., Letcher, B.H., Nislow, K.H. (2008) CREATE: a software to create input files
1112 from diploid genotypic data for 52 genetic software programs. *Molecular Ecology*
1113 *Resources*, **8**, 578-580.

1114 Cornuet, J.M., Luikart, G. (1996) Description and power analysis of two tests for detecting
1115 recent population bottlenecks from allele frequency data. *Genetics*, **144**, 2001-2014.

1116 Cuisance, D. (1995) *Réactualisation de la situation des tsé-tsés et des trypanosomoses*
1117 *animales au Tchad. Enquête réalisée du 9 février au 18 mars 1995*, Maisons-Alfort :
1118 CIRAD-EMVT ed. Maisons-Alfort : CIRAD-EMVT, Maison-Alfort.

1119 Cuisance, D., Février, J., Déjardin, J., Filledier, J. (1985) Dispersion linéaire de *Glossina*
1120 *palpalis gambiensis* et *G. tachinoides* dans une galerie forestière en zone soudano-

Mis en forme : Français (France)

Mis en forme : Français (France)

1121 guinéenne (Burkina Faso). *Revue d'Elevage et de Médecine Vétérinaire des Pays*
1122 *Tropicaux*, **38**, 153-172.

1123 De Meeûs, T. (2012) *Initiation à la génétique des populations naturelles: Applications aux*
1124 *parasites et à leurs vecteurs*. IRD Editions, Marseille.

1125 De Meeûs, T. (2014) Statistical decision from k test series with particular focus on
1126 population genetics tools: a DIY notice. *Infection Genetics and Evolution*, **22**, 91-93.

1127 De Meeûs, T. (2018) Revisiting F_{IS} , F_{ST} , Wahlund effects, and Null alleles. *Journal of*
1128 *Heredity*, **109**, 446-456. 10.1093/jhered/esx106

1129 De Meeûs, T., Chan, C.T., Ludwig, J.M., Tsao, J.I., Patel, J., Bhagatwala, J., Beati, L.
1130 (2021) Deceptive combined effects of short allele dominance and stuttering: an example
1131 with *Ixodes scapularis*, the main vector of Lyme disease in the U.S.A. *Peer Community*
1132 *Journal*, **1**, e40. <https://doi.org/10.24072/pcjournal.34>

1133 De Meeûs, T., Goudet, J. (2007) A step-by-step tutorial to use HierFstat to analyse
1134 populations hierarchically structured at multiple levels. *Infection Genetics and Evolution*, **7**,
1135 731-735.

1136 De Meeûs, T., Guégan, J.F., Teriokhin, A.T. (2009) MultiTest V.1.2, a program to
1137 binomially combine independent tests and performance comparison with other related
1138 methods on proportional data. *BMC Bioinformatics*, **10**, 443.

1139 De Meeûs, T., Humair, P.F., Grunau, C., Delaye, C., Renaud, F. (2004) Non-Mendelian
1140 transmission of alleles at microsatellite loci: an example in *Ixodes ricinus*, the vector of
1141 Lyme disease. *International Journal for Parasitology*, **34**, 943-950.

1142 De Meeûs, T., Koffi, B.B., Barré, N., de Garine-Wichatitsky, M., Chevillon, C. (2010) Swift
1143 sympatric adaptation of a species of cattle tick to a new deer host in New-Caledonia.
1144 *Infection Genetics and Evolution*, **10**, 976-983.

1145 De Meeûs, T., McCoy, K.D., Prugnolle, F., Chevillon, C., Durand, P., Hurtrez-Boussès, S.,
1146 Renaud, F. (2007) Population genetics and molecular epidemiology or how to "débusquer
1147 la bête". *Infection Genetics and Evolution*, **7**, 308-332.

1148 De Meeûs, T., Ravel, S., Solano, P., Bouyer, J. (2019) Negative density dependent
1149 dispersal in tsetse flies: a risk for control campaigns? *Trends in Parasitology*, **35**, 615-621.

1150 Do, C., Waples, R.S., Peel, D., Macbeth, G.M., Tillett, B.J., Ovenden, J.R. (2014)
1151 NeEstimator v2: re-implementation of software for the estimation of contemporary effective
1152 population size (N_e) from genetic data. *Molecular Ecology Resources*, **14**, 209-214.
1153 10.1111/1755-0998.12157

1154 Fox, J. (2005) The R commander: a basic statistics graphical user interface to R. *Journal*
1155 *of Statistical Software*, **14**, 1–42.

1156 Fox, J. (2007) Extending the R commander by "plug in" packages. *R News*, **7**, 46–52.

1157 Frontier, S. (1976) Etude de la décroissance des valeurs propres dans une analyse en
1158 composantes principales: comparaison avec le modèle du bâton brisé. *Journal of*
1159 *Experimental Marine Biology and Ecology*, **25**, 67-75.

1160 Gimonneau, G., Ouedraogo, R., Salou, E., Rayaisse, J.-B., Buatois, B., Solano, P.,
1161 Dormont, L., Roux, O., Bouyer, J. (2021) Larviposition site selection mediated by volatile
1162 semiochemicals in *Glossina palpalis gambiensis*. *Ecological Entomology*, **46**, 301-309.
1163 DOI: 10.1111/een.12962

1164 Goudet, J. (1995) FSTAT (Version 1.2): A computer program to calculate F-statistics.
1165 *Journal of Heredity*, **86**, 485-486.

1166 Goudet, J. (2003) Fstat (ver. 2.9.4), a program to estimate and test population genetics
1167 parameters. Available at <http://www.t-de-meeus.fr/Programs/Fstat294.zip>, Updated from
1168 Goudet (1995).

1169 Goudet, J. (2005) HIERFSTAT, a package for R to compute and test hierarchical F-
1170 statistics. *Molecular Ecology Notes*, **5**, 184-186.

Mis en forme : Français (France)

1171 Goudet, J., Perrin, N., Waser, P. (2002) Tests for sex-biased dispersal using bi-parentally
1172 inherited genetic markers. *Molecular Ecology*, **11**, 1103–1114.

1173 Goudet, J., Raymond, M., De Meeûs, T., Rousset, F. (1996) Testing differentiation in
1174 diploid populations. *Genetics*, **144**, 1933-1940.

1175 Gruvel, J. (1966) Les glossines vectrices des trpanosomiasés au Tchad. *Revue d'Élevage*
1176 *et de Médecine Vétérinaire des Pays Tropicaux*, **19**, 169-212.

1177 Guinand, B. (1996) Use of a multivariate model using allele frequency distributions to
1178 analyse patterns of genetic differentiation among populations. *Biological Journal of the*
1179 *Linnean Society*, **58**, 173-195.

1180 Hargrove, J.W., Vale, G.A. (1979) Aspects of the feasibility of employing odor-baited traps
1181 for controlling tsetse flies (Diptera, Glossinidae). *Bulletin of Entomological Research*, **69**,
1182 283-290. Doi 10.1017/S0007485300017752

1183 Hedrick, P.W. (2005a) *Genetics of Populations, Third Edition*. Jones and Bartlett
1184 Publishers, Sudbury, Massachusetts.

1185 Hedrick, P.W. (2005b) A standardized genetic differentiation measure. *Evolution*, **59**,
1186 1633-1638.

1187 Hijmans, R.J., Williams, E., Vennes, C. (2019) Package 'geosphere': Spherical
1188 Trigonometry. CRAN, pp. Spherical trigonometry for geographic applications. That is,
1189 compute distances and related measures for angular (longitude/latitude) locations.

1190 Ibrahim, M.A.M., Weber, J.S., Ngomtcho, S.C.H., Signaboubo, D., Berger, P., Hassane,
1191 H.M., Kelm, S. (2021) Diversity of trypanosomes in humans and cattle in the HAT foci
1192 Mandoul and Maro, Southern Chad-A matter of concern for zoonotic potential? *PLoS*
1193 *Neglected Tropical Diseases*, **15**, e0009323. <https://doi.org/10.1371/journal.pntd.0009323>

1194 Jombart, T. (2008) adegenet: a R package for the multivariate analysis of genetic markers.
1195 *Bioinformatics*, **24**, 1403-1405. 10.1093/bioinformatics/btn129

Mis en forme : Français (France)

1196 Jombart, T., Devillard, S., Balloux, F. (2010) Discriminant analysis of principal
1197 components: a new method for the analysis of genetically structured populations. *BMC*
1198 *Genetics*, **11**, 94. Artn 94
1199 10.1186/1471-2156-11-94
1200 Karney, C.F.F. (2013) Algorithms for geodesics. *Journal of Geodesy*, **87**, 43-55.
1201 10.1007/s00190-012-0578-z
1202 Kone, N., Bouyer, J., Ravel, S., Vreysen, M.J.B., Domagni, K.T., Causse, S., Solano, P.,
1203 De Meeûs, T. (2011) Contrasting population structures of two vectors of African
1204 trypanosomoses in Burkina Faso: consequences for control. *PLoS Neglected Tropical*
1205 *Diseases*, **5**, e1217. e1217
1206 10.1371/journal.pntd.0001217
1207 Kumar, S., Stecher, G., Tamura, K. (2016) MEGA7: Molecular evolutionary genetics
1208 analysis version 7.0 for bigger datasets. *Molecular Biology and Evolution*, **33**, 1870-1874.
1209 10.1093/molbev/msw054
1210 Mahamat, M.H., Peka, M., Rayaisse, J.B., Rock, K.S., Toko, M.A., Darnas, J., Brahim,
1211 G.M., Alkatib, A.B., Yoni, W., Tirados, I., Courtin, F., Brand, S.P.C., Nersy, C., Alfaroukh,
1212 I.O., Torr, S.J., Lehane, M.J., Solano, P. (2017) Adding tsetse control to medical activities
1213 contributes to decreasing transmission of sleeping sickness in the Mandoul focus (Chad).
1214 *PLoS Neglected Tropical Diseases*, **11**, e0005792. ARTN e0005792
1215 10.1371/journal.pntd.0005792
1216 Manangwa, O., De Meeûs, T., Grébaud, P., Segard, A., Byamungu, M., Ravel, S. (2019)
1217 Detecting Wahlund effects together with amplification problems : cryptic species, null
1218 alleles and short allele dominance in *Glossina pallidipes* populations from Tanzania.
1219 *Molecular Ecology Resources*, **19**, 757-772. 10.1111/1755-0998.12989
1220 Manly, B.J.F. (1997) *Randomization and Monte Carlo Methods in Biology: Second Edition*.
1221 Chapman & Hall, London.

1222 Meirmans, P.G. (2006) Using the amova framework to estimate a standardized genetic
1223 differentiation measure. *Evolution*, **60**, 2399–2402.

1224 Meirmans, P.G., Hedrick, P.W. (2011) Assessing population structure: F_{ST} and related
1225 measures. *Molecular Ecology Resources*, **11**, 5-18. 10.1111/j.1755-0998.2010.02927.x

1226 Mélachio, T., Tito, Tanekou, Simo, G., Ravel, S., De Meeûs, T., Causse, S., Solano, P.,
1227 Lutumba, P., Asonganyi, T., Njiokou, F. (2011) Population genetics of *Glossina palpalis*
1228 *palpalis* from central African sleeping sickness foci. *Parasites and Vectors*, **4**, 140.

1229 Ndung'u, J.M., Boulangé, A., Picado, A., Mugenyi, A., Mortensen, A., Hope, A., Mollo,
1230 B.G., Bucheton, B., Wamboga, C., Waiswa, C., Kaba, D., Matovu, E., Courtin, F., Garrod,
1231 G., Gimonneau, G., Bingham, G.V., Hassane, H.M., Tirados, I., Saldanha, I., Kabore, J.,
1232 Rayaisse, J.B., Bart, J.M., Lingley, J., Esterhuizen, J., Longbottom, J., Pulford, J.,
1233 Kouakou, L., Sanogo, L., Cunningham, L., Camara, M., Koffi, M., Stanton, M., Lehane, M.,
1234 Kagbadouno, M.S., Camara, O., Bessell, P., Mallaye, P., Solano, P., Selby, R., Dunkley,
1235 S., Torr, S., Biéler, S., Lejon, V., Jamonneau, V., Yoni, W., Katz, Z. (2020) Trypa-NO!
1236 contributes to the elimination of gambiense human African trypanosomiasis by combining
1237 tsetse control with "screen, diagnose and treat" using innovative tools and strategies.
1238 *PLoS Neglected Tropical Diseases*, **14**, e0008738. ARTN e0008738
1239 10.1371/journal.pntd.0008738

1240 Nomura, T. (2008) Estimation of effective number of breeders from molecular coancestry
1241 of single cohort sample. *Evolutionary Applications*, **1**, 462-474.

1242 Pearson, K. (1903) Assortative mating in man: a cooperative study. *Biometrika*, **2**, 481-
1243 498. <https://doi.org/10.2307%2F2331510>

1244 Peel, D., Waples, R.S., Macbeth, G.M., Do, C., Ovenden, J.R. (2013) Accounting for
1245 missing data in the estimation of contemporary genetic effective population size (N_e).
1246 *Molecular Ecology Resources*, **13**, 243-253.

1247 Piry, S., Luikart, G., Cornuet, J.M. (1999) BOTTLENECK: A computer program for
1248 detecting recent reductions in the effective population size using allele frequency data.
1249 *Journal of Heredity*, **90**, 502-503.

1250 Prugnolle, F., De Meeûs, T. (2002) Inferring sex-biased dispersal from population genetic
1251 tools: a review. *Heredity*, **88**, 161-165.

1252 Prugnolle, F., De Meeûs, T. (2010) Apparent high recombination rates in clonal parasitic
1253 organisms due to inappropriate sampling design. *Heredity*, **104**, 135-140.

1254 R-Core-Team (2020) R: A Language and Environment for Statistical Computing, Version
1255 3.6.3 (2020-02-29) ed. R Foundation for Statistical Computing, Vienna, Austria,
1256 <http://www.R-project.org>.

1257 Ravel, S., Rayaisse, J.-B., Courtin, F., Solano, P., De Meeûs, T. (2013) Genetic signature
1258 of a recent southern range shift in *Glossina tachinoides* in East Burkina Faso. *Infection*
1259 *Genetics and Evolution*, **18**, 309-314.

1260 Ravel, S., Sere, M., Manangwa, O., Kagbadouno, M., Mahamat, M.H., Shereni, W.,
1261 Okeyo, W.A., Argiles-Herrero, R., De Meeûs, T. (2020) Developing and quality testing of
1262 microsatellite loci for four species of *Glossina*. *Infection Genetics and Evolution*, **85**,
1263 104515. 10.1016/j.meegid.2020.104515

1264 Rousset, F. (1997) Genetic differentiation and estimation of gene flow from *F*-statistics
1265 under isolation by distance. *Genetics*, **145**, 1219-1228.

1266 Rousset, F. (2008) GENEPOP '007: a complete re-implementation of the GENEPOP
1267 software for Windows and Linux. *Molecular Ecology Resources*, **8**, 103-106.

1268 Saitou, N., Nei, M. (1987) The neighbor-joining method: a new method for reconstructing
1269 phylogenetic trees. *Molecular Biology and Evolution*, **4**, 406-425.

1270 Séré, M., Thévenon, S., Belem, A.M.G., De Meeûs, T. (2017) Comparison of different
1271 genetic distances to test isolation by distance between populations. *Heredity*, **119**, 55-63.
1272 10.1038/hdy.2017.26

1273 She, J.X., Autem, M., Kotulas, G., Pasteur, N., Bonhomme, F. (1987) Multivariate analysis
1274 of genetic exchanges between *Solea aegyptiaca* and *Solea senegalensis* (Teleosts,
1275 Soleidae). *Biological Journal of the Linnean Society*, **32**, 357-371. DOI 10.1111/j.1095-
1276 8312.1987.tb00437.x

1277 Signaboubo, D., Payne, V.K., Moussa, I.M.A., Hassane, H.M., Berger, P., Kelm, S., Simo,
1278 G. (2021) Diversity of tsetse flies and trypanosome species circulating in the area of Lake
1279 Iro in southeastern Chad. *Parasites & Vectors*, **14**, 293. 10.1186/s13071-021-04782-7

1280 Solano, P., Ravel, S., De Meeûs, T. (2010) How can tsetse population genetics contribute
1281 to African trypanosomiasis control? *Trends in Parasitology*, **26**, 255-263.

1282 Takezaki, N., Nei, M. (1996) Genetic distances and reconstruction of phylogenetic trees
1283 from microsatellite DNA. *Genetics*, **144**, 389-399.

1284 Teriokhin, A.T., De Meeûs, T., Guegan, J.F. (2007) On the power of some binomial
1285 modifications of the Bonferroni multiple test. *Zhurnal Obshchei Biologii*, **68**, 332-340.

1286 Thomas, F., Renaud, F., Derothe, J.M., Lambert, A., De Meeûs, T., Cezilly, F. (1995)
1287 Assortative pairing in *Gammarus-Insensibilis* (Amphipoda) Infected by a Trematode
1288 parasite. *Oecologia*, **104**, 259-264.

1289 Traynor, K.S., Mondet, F., de Miranda, J.R., Techer, M., Kowallik, V., Oddie, M.A.Y.,
1290 Chantawannakul, P., McAfee, A. (2020) *Varroa destructor*: a complex parasite, crippling
1291 honey bees worldwide. *Trends in Parasitology*, **36**, 592-606. 10.1016/j.pt.2020.04.004

1292 Vale, G.A., Hursey, B.S., Hargrove, J.W., Torr, S.J., Allsopp, R. (1984) The use of small
1293 plots to study populations of tsetse (Diptera, Glossinidae): difficulties associated with
1294 population dispersal. *Insect Science and its Application*, **5**, 403-410. Doi
1295 10.1017/S1742758400008730

1296 Van Oosterhout, C., Hutchinson, W.F., Wills, D.P.M., Shipley, P. (2004) MICRO-
1297 CHECKER: software for identifying and correcting genotyping errors in microsatellite data.
1298 *Molecular Ecology Notes*, **4**, 535-538.

1299 Vitalis, R. (2002) Estim 1.2-2: a computer program to infer population parameters from
1300 one- and two-locus gene identity probabilities, Available at [http://www.t-de-
1302 meeus.fr/ProgMeeusGB.html](http://www.t-de-
1301 meeus.fr/ProgMeeusGB.html).
1303 Vitalis, R., Couvet, D. (2001a) ESTIM 1.0: a computer program to infer population
1304 parameters from one- and two-locus gene identity probabilities. *Molecular Ecology Notes*,
1305 **1**, 354-356.
1306 Vitalis, R., Couvet, D. (2001b) Estimation of effective population size and migration rate
1307 from one- and two-locus identity measures. *Genetics*, **157**, 911-925.
1308 Vreysen, M.J.B., Balenghien, T., Saleh, K.M., Maiga, S., Koudougou, Z., Cecchi, G.,
1309 Bouyer, J. (2013) Release-Recapture Studies Confirm Dispersal of *Glossina palpalis*
1310 *gambiensis* between River Basins in Mali. *PLoS Neglected Tropical Diseases*, **7**, e2022.
1311 ARTN e2022
1312 10.1371/journal.pntd.0002022
1313 Wahlund, S. (1928) Zusammensetzung von populationen und korrelationsers-chinungen
1314 von standpunkt der vererbungslehre aus betrachtet. *Hereditas*, **11**, 65-106.
1315 Wang, J. (2015) Does G_{ST} underestimate genetic differentiation from marker data?
1316 *Molecular Ecology*, **24**, 3546-3558. 10.1111/mec.13204
1317 Waples, R.S. (2006) A bias correction for estimates of effective population size based on
1318 linkage disequilibrium at unlinked gene loci. *Conservation Genetics*, **7**, 167-184.
1319 Watts, P.C., Rousset, F., Saccheri, I.J., Leblois, R., Kemp, S.J., Thompson, D.J. (2007)
1320 Compatible genetic and ecological estimates of dispersal rates in insect (*Coenagrion*
1321 *mercuriale*: Odonata: Zygoptera) populations: analysis of 'neighbourhood size' using a
1322 more precise estimator. *Molecular Ecology*, **16**, 737-751.
1323 Weir, B.S., Cockerham, C.C. (1984) Estimating F-statistics for the analysis of population
1324 structure. *Evolution*, **38**, 1358-1370.

- 1324 Werren, J.H. (1980) Sex ratio adaptations to local mate competition in a parasitic wasp.
1325 *Science*, **208**, 1157-1159. 10.1126/science.208.4448.1157
- 1326 Wright, S. (1965) The interpretation of population structure by F-statistics with special
1327 regard to system of mating. *Evolution*, **19**, 395-420.
- 1328 Yang, R.C. (1998) Estimating hierarchical *F*-statistics. *Evolution*, **52**, 950-956.
1329
1330

1331 **APPENDICES**

1332

1333 **Appendix 1: Example of scripts to compute geographic distances or surfaces with**
1334 **the R package geosphere**

```
1335 # to compute geographic distance (in meters) with GPPS coordinate in decimal
1336 # degrees: long1 and lat1, and long2 and lat2 for the coordinates of points 1
1337 # and 2 respectively.
1338
1339 distGeo(c(long1,lat1),c(long2, lat2))
1340
1341 #With two files with two columns (longitude and latitude), the first file
1342 #containing the GPS coordinates of the first point of site pairs, and the second
1343 #file containing the corresponding GPS coordinates of the second point of site
1344 #pairs.
1345
1346 LongLat1 <- read.table("Long1Lat1.txt", header=TRUE, stringsAsFactors=TRUE,
1347 sep="\t", na.strings="NA", dec=".", strip.white=TRUE)
1348 LongLat2 <- read.table("Long2Lat2.txt", header=TRUE, stringsAsFactors=TRUE,
1349 sep="\t", na.strings="NA", dec=".", strip.white=TRUE)
1350 distGeo(LongLat1,LongLat2)
1351
1352 # To compute the area of a polygon in angular coordinates (longitude/latitude)
1353 #on an ellipsoid.
1354 #Dataset has two columns : Longitude and Latitude
1355 Dataset <- read.table("MyData.txt", header=TRUE, stringsAsFactors=TRUE,
1356 sep="\t", na.strings="NA", dec=".", strip.white=TRUE)
1357 attach(Dataset)
1358 areaPolygon(data.frame(Longitude,Latitude))
1359
```

1360 **Appendix 2: Script and results for the HierFstat analysis**

1361 For Mandoul

```
1362 > data<-read.table("MandoulHier.txt",header=TRUE)
1363 > attach(data)
1364 > loci<-
1365 data.frame(Locus1,Locus2,Locus3,Locus4,Locus5,Locus6,Locus7,Locus8,Locus9)
1366 > levels<-data.frame(Site,Subsite,Trap)
1367 > varcomp.glob(levels,loci)
1368 $F
1369           Site      Subsite      Trap      Ind
1370 Total  0.0004076288 0.01821699 -0.008157967 0.1326307
1371 Site    0.0000000000 0.01781663 -0.008569089 0.1322770
```

Mis en forme : Français (France)


```

1372 Subsite 0.0000000000 0.00000000 -0.026864347 0.1165367
1373 Trap 0.0000000000 0.00000000 0.000000000 0.1396494
1374 > test.within(loci,test=Trap,within=Subsite,nperm=1000)
1375 $p.val
1376 [1] 0.72
1377 > test.between.within(loci,within=Site,rand.unit=Trap,test=Subsite,nperm=1000)
1378 $p.val
1379 [1] 0.025
1380
1381 > test.between(loci,rand.unit=Subsite,test=Site,nperm=1000)
1382 $p.val
1383 [1] 0.303
1384
1385 For Maro
1386 > data<-read.table("MaroT0Hier.txt",header=TRUE)
1387 > attach(data)
1388 > loci<-
1389 data.frame(Locus1,Locus2,Locus3,Locus4,Locus5,Locus6,Locus7,Locus8,Locus9)
1390 > levels<-data.frame(Site,Subsite,Trap)
1391 > varcomp.glob(levels,loci)
1392 $F
1393
1394      Site      Subsite      Trap      Ind
1395 Total -0.006634284 -0.006208540 -0.001297964 0.07391164
1396 Site 0.000000000 0.000422938 0.005301150 0.08001508
1397 Subsite 0.000000000 0.000000000 0.004880276 0.07962582
1398 Trap 0.000000000 0.000000000 0.000000000 0.07511211
1399 > test.within(loci,test=Trap,within=Subsite,nperm=1000)
1400 $p.val
1401 [1] 0.031
1402
1403 > test.between.within(loci,within=Site,rand.unit=Trap,test=Subsite,nperm=1000)
1404 $p.val
1405 [1] 0.656
1406
1407 > test.between(loci,rand.unit=Subsite,test=Site,nperm=1000)
1408 $p.val
1409 [1] 0.567
1410
1411 For Timbéri and Dokoutou
1412 > data<-read.table("TimberiDokoutouHier.txt",header=TRUE)
1413 > attach(data)

```

```

1414 > loci<-
1415 data.frame(Locus1,Locus2,Locus3,Locus4,Locus5,Locus6,Locus7,Locus8,Locus9)
1416 > levels<-data.frame(Zone,Subsite,Trap)
1417 > varcomp.glob(levels,loci)
1418 $F
1419      Zone      Subsite      Trap      Ind
1420 Total  0.07493418 0.09378198 0.0754573949 0.15831925
1421 Zone   0.00000000 0.02037454 0.0005655925 0.09013960
1422 Subsite 0.00000000 0.00000000 -0.0202209403 0.07121605
1423 Trap   0.00000000 0.00000000 0.0000000000 0.08962470
1424
1425 > test.within(loci,within=Subsite,test=Trap,nperm=1000)
1426 $p.val
1427 [1] 0.961
1428
1429 > test.between.within(loci,within=Zone,rand.unit=Trap,test=Subsite,nperm=1000)
1430 $p.val
1431 [1] 0.66
1432
1433 > test.between(loci,rand.unit=Subsite,test=Zone,nperm=1000)
1434 0.196
1435
1436 Timbéri and Doukoutou without subsites
1437 > data<-read.table("TimberiDokoutouHier.txt",header=TRUE)
1438 > attach(data)
1439 > loci<-
1440 data.frame(Locus1,Locus2,Locus3,Locus4,Locus5,Locus6,Locus7,Locus8,Locus9)
1441 > levels<-data.frame(Zone,Trap)
1442 > varcomp.glob(levels,loci)
1443 $loc
1444      [,1]      [,2]      [,3]      [,4]
1445 Locus1 -0.005416145 0.049552374 0.11500959 0.3913043
1446 Locus2 0.079303509 -0.036826228 -0.04782076 0.9130435
1447 Locus3 0.025164936 -0.048459828 0.15830136 0.6956522
1448 Locus4 0.094947329 -0.026895027 0.09454775 0.5777778
1449 Locus5 0.073639708 0.010224110 0.19631820 0.2826087
1450 Locus6 0.069050675 -0.019157955 0.18475597 0.5434783
1451 Locus7 0.102895393 -0.026648790 -0.02472293 0.8043478
1452 Locus8 0.100433760 0.004003843 -0.02738751 0.8222222
1453 Locus9 0.073513023 0.008805412 -0.06188017 0.9333333
1454

```

Mis en forme : Anglais (États-Unis)

Mis en forme : Français (France)

Mis en forme : Anglais (États-Unis)

Mis en forme : Français (France)

```

1455 $overall
1456     Zone      Trap      Ind      Error
1457 0.61353219 -0.08540209 0.58712151 5.96376812
1458
1459 $F
1460     Zone      Trap      Ind
1461 Total 0.08666909 0.07460498 0.15754323
1462 Zone 0.00000000 -0.01320892 0.07759963
1463 Trap 0.00000000 0.00000000 0.08962470
1464
1465 > test.between(loci,rand.unit=Trap,test=Zone,nperm=1000)
1466 $p.val
1467 [1] 0.004
1468
1469 This shows that without Subsites, Zone becomes significant
1470
1471 Dokoutou and Timbéri without Traps
1472 > data<-read.table("TimberiDokoutouHier.txt",header=TRUE)
1473 > attach(data)
1474
1475 > levels<-data.frame(Zone,Subsite)
1476 > varcomp.glob(levels,loci)
1477 $F
1478     Zone      Subsite      Ind
1479 Total 0.07704913 0.08702932 0.15810591
1480 Zone 0.00000000 0.01081335 0.08782351
1481 Subsite 0.00000000 0.00000000 0.07785200
1482
1483 > test.within(loci,test=Subsite,within=Zone,nperm=1000)
1484 $p.val
1485 [1] 0.648
1486
1487 > test.between(loci,rand.unit=Subsite,test=Zone,nperm=1000)
1488 $p.val
1489 [1] 0.186
1490
1491 This show that, without traps, Subsite stays non-significant.
1492

```

Mis en forme : Français (France)

1493 **Appendix 3: Detailed analyses of quality testing of genetic markers and sampling**

1494

1495 In dioecious species as tsetse flies, heterozygote deficits can occur as a result of
1496 amplification problems (null alleles, short allele dominance, stuttering or allelic dropouts),
1497 under-dominant selection, assortative mating, systematic breeding between relatives (sib
1498 mating) and Wahlund effect.

1499 Null alleles occur when a particular kind of allele cannot be amplified and then
1500 appears homozygous for the other allele with which it is heterozygous, or as a missing
1501 data when homozygous itself. In case of null alleles, we expect that
1502 $\text{StdrdErrFIS} \geq 2 \times \text{StdrdErrFST}$, a positive correlation between F_{IS} and F_{ST} across loci, and a
1503 positive correlation between the number of missing genotypes (N_{blanks}) and F_{IS} across loci
1504 (De Meeûs, 2018). We tested these correlations with `rcmdr` (one-sided Spearman's rank
1505 correlation tests). We also undertook the regression $F_{IS} \sim N_{\text{blanks}}$, where the determination
1506 coefficient provided a proxy of the percentage of variance of F_{IS} explained by null alleles,
1507 and where the intercept provides a proxy of the "true" F_{IS} in absence of null alleles. Null
1508 allele frequencies were estimated with Brookfield's second method (Brookfield, 1996) with
1509 `MicroChecker` (Van Oosterhout et al., 2004). We used these to estimate the total expected
1510 number of missing genotypes per locus ($N_{\text{blanks-expected}}$) and when useful, compared it to
1511 N_{blanks} with a one-sided (less) exact binomial test under R (command `binom.test`).

1512 Short allele dominance (SAD) occurs when competition for the Taq polymerase
1513 favors the shortest allele in a heterozygote individual (De Meeûs et al., 2004). It was tested
1514 with a one sided (negative correlation) Spearman's rank correlation between F_{IT} and allele
1515 size (Manangwa et al., 2019). In case of doubt, we validated the result with a linear
1516 regression $F_{IS} \sim \text{Allele size}$ weighted by $p_i(1-p_i)$ (De Meeûs et al., 2004), where p_i is the
1517 frequency of allele i . These tests were undertaken with `rcmdr`.

1518 Stuttering is the result of inaccurate PCR amplification through Taq slippage of a
1519 specific DNA strand. This generates several PCR products that differ from each other by
1520 one repeat and can cause difficulties when discriminating homozygotes and individuals
1521 that are heterozygous for alleles with a single repeat difference. The presence of stuttering
1522 was detected with the graphic output of `MicroChecker`. As recommended (De Meeûs et al.,
1523 2021), we considered that the observed deficit of heterozygous individuals for one repeat
1524 difference was a likely consequence of stuttering (we ignored the comments panel that
1525 happened to contradict the graphic in some instances) and set the randomization at the
1526 maximum value (10000). We tried to correct loci with stuttering as in (De Meeûs et al.,
1527 2021): Alleles that are close in size were pooled into one synthetic allele, providing that

1528 one of these alleles has a frequency $p \geq 0.05$, in order to avoid giving too much weight to a
1529 collection of rare alleles. If all alleles are one repeat difference, we tried pooling alleles two
1530 by two. If close alleles are all rare, we did not pool those. These corrections were kept only
1531 for the loci for which F_{IS} of corrected data displayed a decrease as compared to the
1532 uncorrected data.

1533 Underdominance is a process that affects loci where the heterozygous individuals
1534 are less fit than all homozygous genotypes. This phenomenon must be very rare because it
1535 induces a rapid elimination of the rarest alleles, since rare alleles are mostly found
1536 heterozygous. The only documented example is the Rhesus system Rh-/Rh-, where
1537 heterozygous fetuses carried by mothers that are homozygous for Rh- are strongly
1538 disfavored (see for example the book from Hedrick page 180 (Hedrick, 2005a)). The rarity
1539 of such systems, is explained by the fact that rare alleles, which are mostly found in
1540 heterozygous individuals, tend to be rapidly eliminated from populations. Underdominance
1541 is thus highly unlikely to be found associated with a microsatellite marker.

1542 Assortative pairing occurs when individuals mate according to their genotype:
1543 carrier of a given allele prefer to mate with those that carry the same allele. This kind of
1544 systems are not expected to be frequently met in nature as it strongly disfavors the rarest
1545 alleles. There are however some examples with complex determinisms as assortative
1546 mating for size or assortative mating for parasite load (Pearson, 1903; Thomas et al.,
1547 1995). Again, microsatellite markers should not be concerned.

1548 Systematic breeding between relatives occurs when individuals mate preferentially
1549 between relatives as sib mating, due to constraints of life cycles like in some arthropods
1550 like *Nasonia* parasitoid wasps (Werren, 1980) or *Varroa* mites (Traynor et al., 2020).

1551 Wahlund effect (Wahlund, 1928; De Meeûs, 2018) corresponds to a population
1552 genetics syndrome coming from the admixture of individuals from different subpopulations
1553 that do not share the same allele frequencies into the same sample. It produces
1554 heterozygote deficits as compared to Hardy-Weinberg expected genotypic proportions,
1555 and also affects linkage disequilibrium between loci, positively or negatively so, depending
1556 on the initial genetic structure of the different subsamples (Prugnolle & De Meeûs, 2010).

1557

1558 *In Mandoul*

1559 Taking subsites as subpopulation units, only one LD test was significant (p -
1560 value=0.0446), which did not stay significant after BY correction (p -value=1). The global
1561 $F_{IS}=0.128$ in 95%CI=[0.039, 0.243], was significantly different from 0 (p -value<0.0002).
1562 Population structure was weak, with a small and marginally not significant $F_{ST}=0.005$ in

1563 95%CI=[-0.007, 0.016] (p -value=0.0722). Interestingly, F_{IT} =0.132 in 95%CI=[0.047, 0.244]
1564 was not significantly different from the F_{IS} (p -value=0.2129). It is thus possible that the
1565 whole focus behaves as a single population.

1566 Using criteria defined in previous works (De Meeûs, 2018; Manangwa et al., 2019;
1567 De Meeûs et al., 2021), null alleles explained well observed heterozygote deficits. Indeed,
1568 $StdErrFIS$ was 10 times $StdErrFST$, and the correlation between missing data and F_{IS}
1569 was significant (ρ =0.661, p -value=0.0263) with a regression's R^2 =0.55. With F_{IT} , the
1570 relationship improved (ρ =0.6738, p -value=0.0233, R^2 =0.5795). Using F_{IS} or F_{IT}
1571 regressions, the intercept was used to estimate the residual values in absence of null
1572 alleles, which were F_{IS_res} =-0.0547 and F_{IT_res} =-0.0474. No signature of SAD (smaller p -
1573 value=0.175), or of stuttering could be detected. Null alleles average frequency was
1574 around p_{nulls} =0.177 with Brookfield's second method (MicroChecker).

1575 There was no evidence of any Wahlund effect.

1576

1577 *In Maro*

1578 Only one locus pair displayed a marginally significant LD (p -value=0.0444), which
1579 did not stay significant after BY correction (p -value=1).

1580 There was a highly significant heterozygote deficit within traps in that focus:
1581 F_{IS} =0.091 in 95%CI=[0.026, 0.164]. Interestingly, the F_{IT} was smaller than F_{IS} : F_{IT} =0.088 in
1582 95%CI=[0.020, 0.162], but not significantly so (p -value=0.1548, two-sided Wilcoxon signed
1583 rang test for paired data). This is due to a global negative F_{ST} =-0.005 in 95%CI=[-0.01,
1584 0.001] (p -value=0.3363). We thus considered the whole focus as a single population.
1585 Doing so, the within focus F_{IS} =0.088 in 95%CI=[0.021, 0.163], which is smaller than the
1586 within traps F_{IS} , but again, not significantly so (p -value=0.1379, two-sided test). There was
1587 thus potentially a free migration within this focus, and in particular between the most
1588 distant traps that captured tsetse flies that were 33 km distant from each other's.

1589 Within traps, $StdErrFIS$ was 12 times $STdErrFST$, and there was a positive
1590 correlation between F_{IS} and F_{ST} (ρ =0.2176, p -value=0.2869), which suggests the existence
1591 of null alleles. Within the whole focus, the observed F_{IS} was poorly explained by missing
1592 data (ρ =0.11, p -value=0.389). No significant SAD signature could be found at any locus
1593 (all p -values>0.1478). According to Brookfield's second method, null alleles frequencies
1594 explain well the observed F_{IS} and missing data (all p -values>0.5). Additionally, there was a
1595 highly significant signature of stuttering (p -value<0.01) for locus Gff18. Stuttering detection
1596 is not very powerful and null alleles do not explain very well the observed F_{IS} . We thus
1597 tried to correct stuttering for all loci that displayed a deficit in heterozygosity for alleles with

1598 one repeat difference: Gff3, Gff4, Gff12, Gff16, Gff18 and Gff27, following the rules
1599 described in (De Meeûs et al., 2021). For locus Gff3, we pooled allele 196 to 202 into one
1600 allele and the same for 214-218; for locus Gff4, we pooled alleles 140-152 and 156-172;
1601 for locus Gff12, we pooled 137 with 139 and 143-155; for locus 16, 156-166; for locus 18,
1602 212 with 214 and 220-228; and for locus Gff27, 167 with 169 and 187-207. The
1603 consequences of this new coding and possible cure of stuttering effects were first explored
1604 on F_{IS} within traps. The correction improved the results for locus Gff3 (-0.031 before, -
1605 0.119 after), for Gff12 (0.108 before, 0.024 after), for Gff16 (0.267 before, 0.067 after), for
1606 Gff18 (0.269 before, -0.161 after), and for Gff27 (0.173 before, -0.051 after). Stuttering
1607 correction had no effect on Gff4 (0.025 before, 0.044 after). We thus kept these stuttering
1608 recoding for all loci but Gff4 for further analyses.

1609 There was no evidence of any Wahlund effect.

1610

1611 *In Dokoutou and Timbéri*

1612 Given the results obtained with the hierarchical analysis, we took directly the whole
1613 zones as subpopulation units, except when specified otherwise.

1614 Within the two zones, only one pair of loci appeared in significant linkage (p -
1615 value=0.0307), which did not stay significant after BY correction (p -value=1). There was a
1616 substantial and highly significant heterozygote deficit, $F_{IS}=0.08$ in 95%CI=[-0.011, 0.191]
1617 (p -value=0.0028). It was in fact smaller, but not significantly so, than the $F_{IS}=0.09$ in
1618 95%CI=[0.001, 0.196] measured within traps (p -value=0.4258, two-sided test). The site
1619 was thus probably the correct subpopulation scale. The standard error of F_{IS} was four
1620 times the one of F_{ST} , which suggested the presence of null alleles or other amplification
1621 problems. The correlation between F_{IS} and F_{ST} was weak and not significant ($\rho=0.1255$, p -
1622 value=0.3738). The correlation between F_{IS} and the number of missing genotypes was
1623 negative ($\rho=-0.3651$, p -value=0.8331). However, with three blank genotypes there was
1624 little opportunity to find anything. No significant signature of SAD could be found (smallest
1625 p -value=0.1332). According to Brookfield's second method, missing data were enough to
1626 explain the observed heterozygote deficit with null alleles (smallest p -value=0.4242). But
1627 again, subsample sizes may not have been big enough. Stuttering was significant for
1628 Gff16 and Gff18 in Dokoutou. Given the low power of the detection procedures, we tried to
1629 correct for stuttering for all loci with heterozygote deficits: Gff3 ($F_{IS}=0.281$), Gff8
1630 ($F_{IS}=0.148$), Gff12 ($F_{IS}=0.113$), Gff16 ($F_{IS}=0.419$) and Gff18 ($F_{IS}=0.238$). For Gff3, we
1631 pooled alleles 202 and 204 with 200; for Gff8, 160 with 158, 176 to 182 with 174, and 192
1632 with 190; for Gff12, 145 with 143, and 151 and 153 with 149; for Gff16, 158 with 156, and

1633 162-166 with 160; and for Gff18, 224 with 222, 234-238 with 232, and 244 with 242. The
 1634 results was very good for Gff8 ($F_{IS}=0.018$), Gff12 ($F_{IS}=0.001$) and Gff18 ($F_{IS}=0.035$), but
 1635 very bad for Gff3 ($F_{IS}=0.331$) and Gff16 ($F_{IS}=643$). We thus further kept stuttering
 1636 correction for Gff8, Gff12 and Gff18 only.

1637 Four locus pairs appeared in significant LD (smallest p -value=0.0282), none of
 1638 which stayed significant after BY correction (all p -values=1). The heterozygote deficit
 1639 ($F_{IS}=0.031$) was not significant any more (p -value=0.2906). The standard error of F_{IS} was
 1640 still four times the one of F_{ST} , suggesting some kind of amplification problems at some loci,
 1641 which are not very well explained by null alleles (correlations between F_{IS} and F_{ST} or
 1642 number of missing genotypes were both negative). Nevertheless, Gff3 and Gff16, that did
 1643 not display any missing genotype, could be explained by null alleles according to
 1644 Brookfield's second method, with frequencies 0.09 and 0.14 (p -value=0.6868 and p -
 1645 value=0.4242), for Gff3 and Gff16 respectively.

1646 There was no evidence of any Wahlund effect.

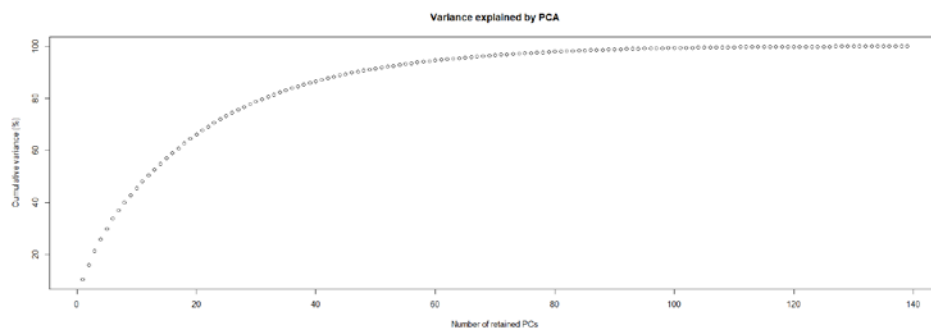
1647

1648 **Appendix 4: script, outputs and discussion for the DAPC analysis of *Glossina***

1649 ***fuscipes fuscipes* from southern Chad, with the R package adegenet**

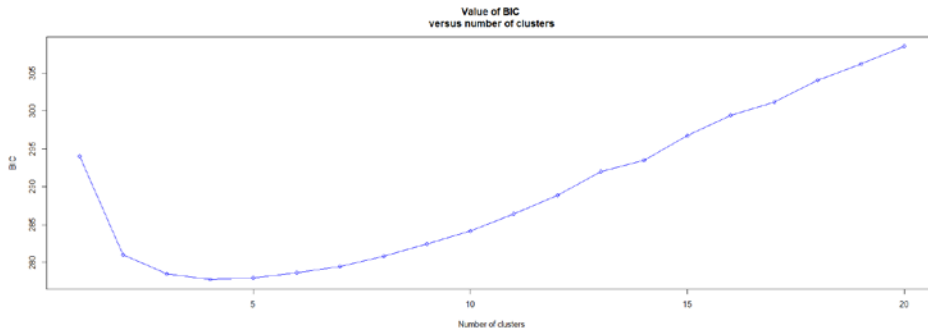
1650 *Scripts and outputs*

```
1651 > GffChadSpatial<-read.table("GffChadSpatialTrapsDAPC.txt", header=TRUE,
1652 sep="\t", na.strings="NA", dec=".", strip.white=TRUE)
1653 > GffChadSpatialADE<-df2genind(GffChadSpatial, sep = NULL, ncode = 3, ind.names
1654 = NULL, loc.names = NULL, pop = NULL, NA.char = "NA", ploidy = 2, type =
1655 "codom", strata = NULL, hierarchy = NULL)
1656 > x<-GffChadSpatialADE
1657 > grp<-find.clusters(x,max.n.clust=20)
```



1658

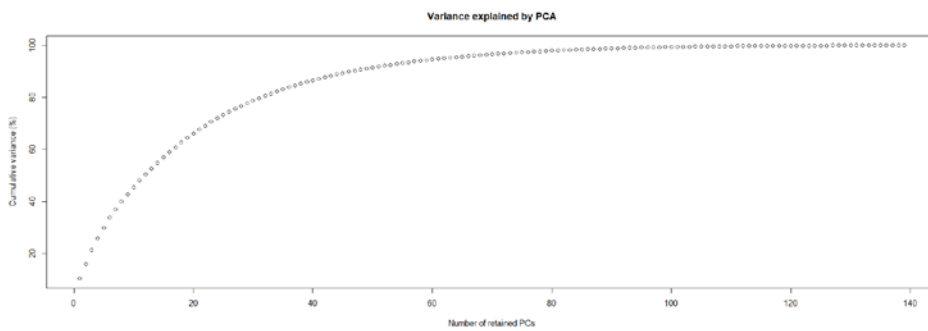
1659 Choose the number PCs to retain (≥ 1): 100



```

1660
1661 Choose the number of clusters (>=2): 4
1662 > dapcl <- dapc(x, grp$grp,n.pca= NULL, n.da= NULL, var.contrib = TRUE, scale =
1663 FALSE)

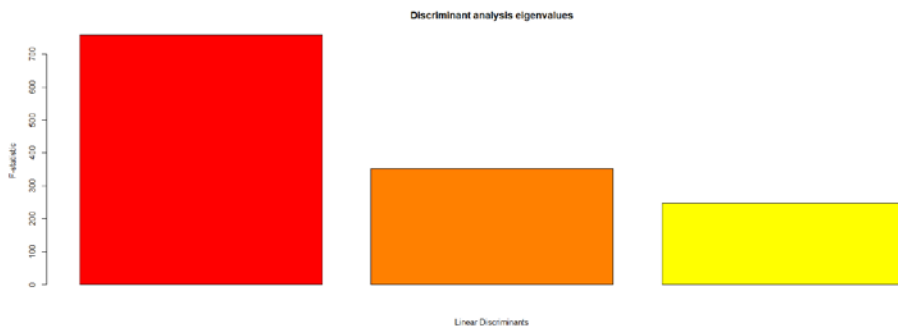
```



```

1664
1665 Choose the number PCs to retain (>=1): 100

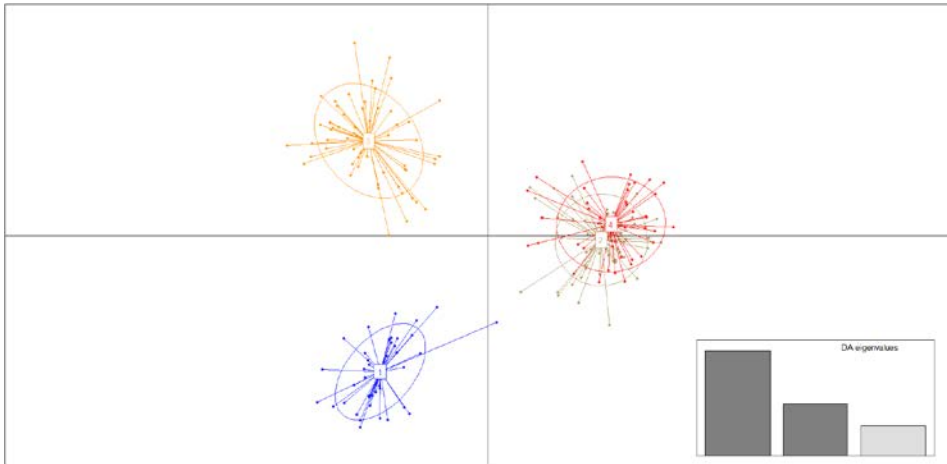
```



```

1666
1667 Choose the number discriminant functions to retain (>=1): 3
1668 scatter(dapcl)

```



```

1669
1670 > summary(dapcl)
1671 $n.dim
1672 [1] 3
1673
1674 $n.pop
1675 [1] 4
1676
1677 $assign.prop
1678 [1] 1
1679
1680 $assign.per.pop
1681 1 2 3 4
1682 1 1 1 1
1683
1684 $prior.grp.size
1685 1 2 3 4
1686 44 57 60 44
1687
1688
1689 $post.grp.size
1690 1 2 3 4
1691 44 57 60 44
1692
1693 > tabGffChadSpatial<-data.frame(Cluster=c(grp$grp),Proportion_assign_cluster
1694 =dapcl$posterior,geno=GffChadSpatial)
1695 > write.table(tabGffChadSpatial,"tabGffChadSpatialTDAPCResK4.txt",col=NA,
1696 sep="\t", dec=".")
1697 > write.table(dapcl$ind.coord, "CoordDAPC.txt", sep="\t")

```

```
1698 > write.table(dapc1$means, "GroupMeansDAPC.txt", sep="\t")
1699 > write.table(dapc1$grp.coord, "GroupCoordDAPC.txt", sep="\t")
```

1700

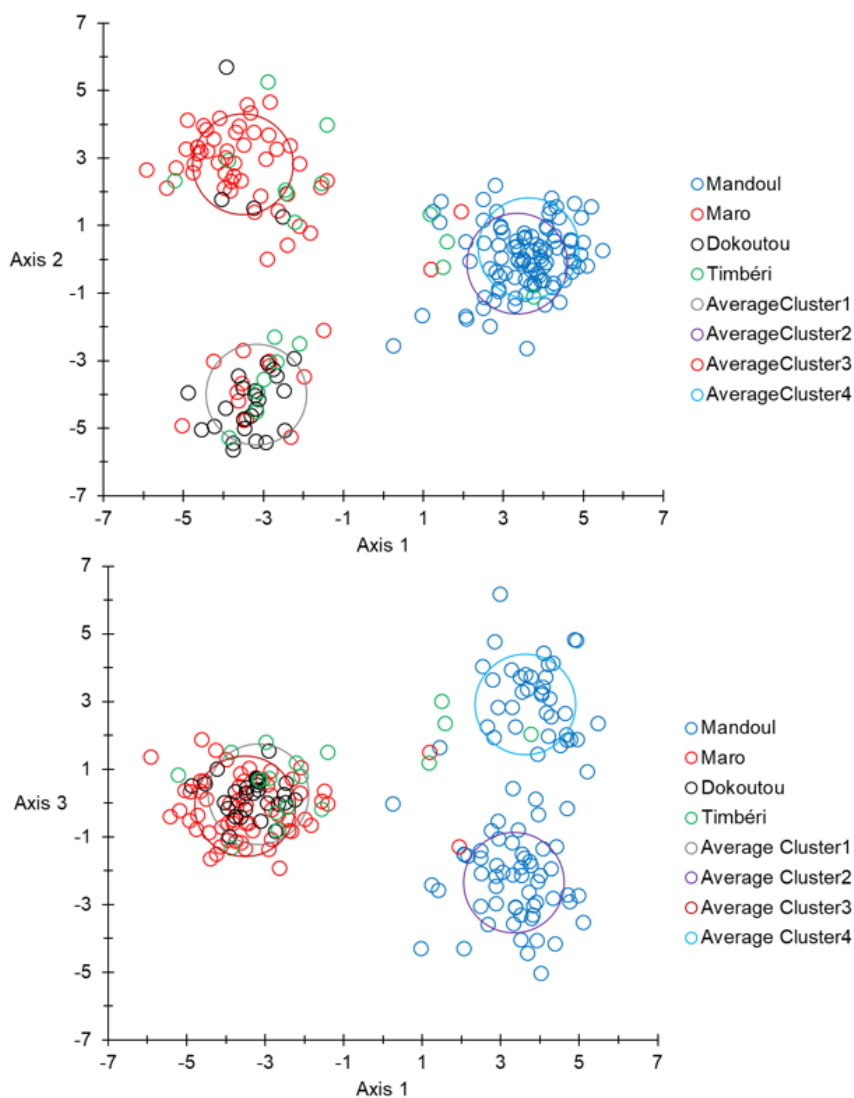
1701 *Results and discussion*

1702 The optimal partition consisted of four clusters (as the number of samples), with a
1703 strong average assignment (~1), but containing admixtures of individuals from different
1704 zones, even if some clusters contained more individuals from particular zones than others
1705 (Figure A1).

1706 Combined effects of occasional exchange, isolation by distance, temporal effects
1707 and amplification issues probably explain why the DAPC analysis provided hardly
1708 interpretable results. This challenges the relevance of this approach in some instances,
1709 but this would require further new theoretical approaches.

1710

1711 Figure A1: Projection on the two first axes (top) and axes 1 and 3 (bottom) of the DAPC
 1712 analyses of individuals of *Glossina fuscipes fuscipes* from Southern Chad. The
 1713 belonging to a particular focus/site are represented by different colors. Averages of
 1714 the four clusters are symbolized by big circles of different colors. Mandoul flies
 1715 belong to cohort 1, Maro to cohort 22 and Dokoutou and Timbéri to cohort 32.



1716
 1717
 1718